GEOCHEMICAL TRACING OF THE SOURCE OF WATER DISSOLVED INORGANIC CARBON AND CHLORIDE IN BANKS PENINSULA WARM SPRINGS, NEW ZEALAND

A THESIS SUBMITTED IN PARTIAL FULFILMENT

OF THE REQUIREMENTS FOR THE DEGREE OF

MASTER OF SCIENCE IN GEOLOGY

AT THE

DEPARTMENT OF GEOLOGICAL SCIENCES

UNIVERSITY OF CANTERBURY

BY SAMANTHA NICOLE GRIFFIN

UNIVERSITY OF CANTERBURY

2016

FRONTISPIECE

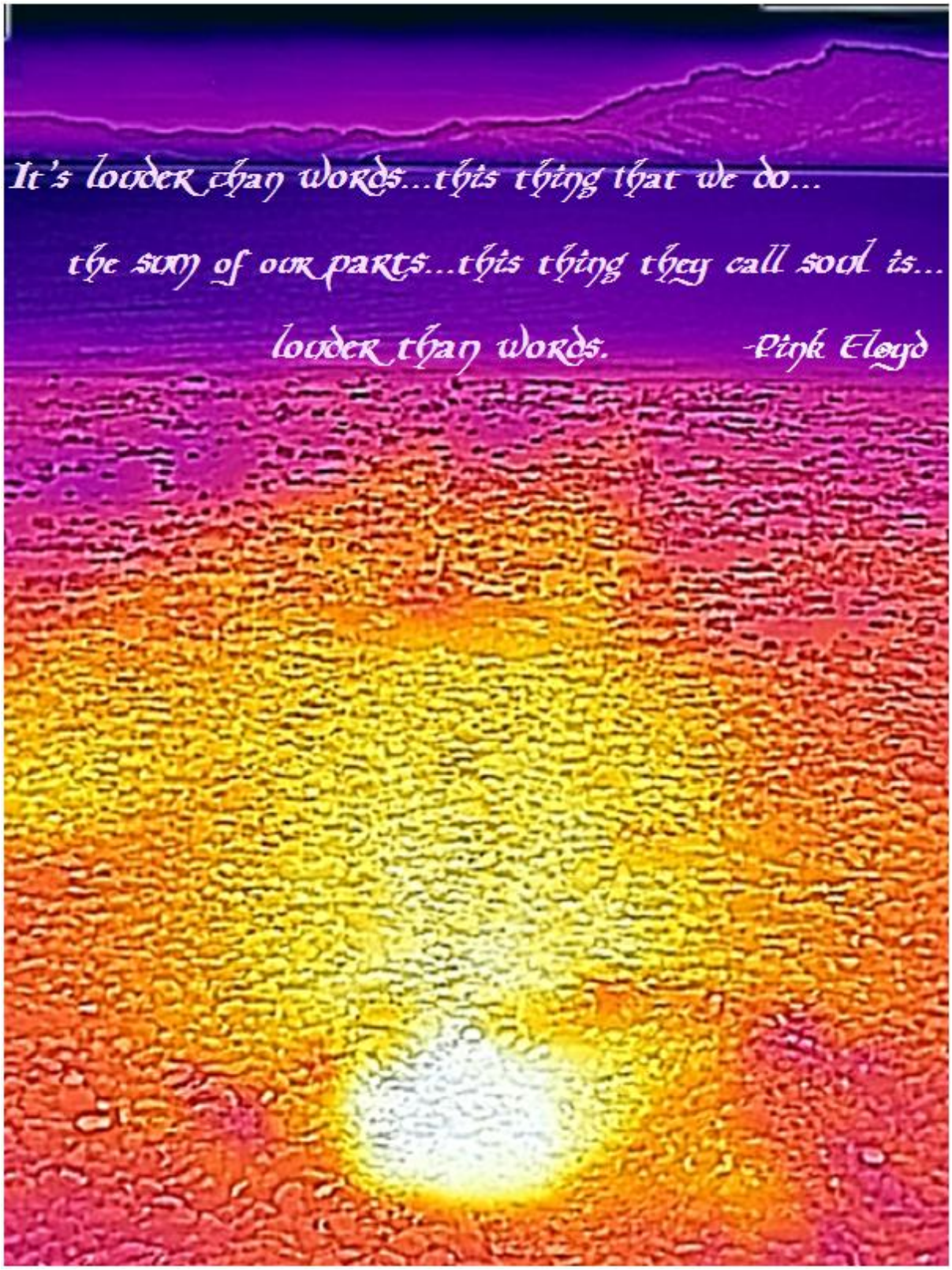

32 °C warm spring of Rapaki Bay, Banks Peninsula, discharging into Lyttelton Harbour at mid-tide, 25/03/2015.

ABSTRACT

Determining the source, transport and fate or crustal fluids is an important problem in modern geoscience. Crustal fluids affect rheology and rock deformation through water-rock interaction at elevated temperatures and pressures. Geothermal resources are a globally significant source of low-carbon energy, and their associated hydrothermal systems are responsible for the formation of most of the world's precious metal deposits. Knowing where fluids originate in the crust, what flow paths they follow, and the conditions under which they discharge to the surface is essential to understanding how rocks, water and volatiles interact. This thesis explores the low-enthalpy warm springs present on Banks Peninsula, New Zealand, an anomalous and understudied example of upper-crustal fluid flow in one of the world's most active orogens. Geochemical tracing of the water in conjunction with soil-gas flux surveying has been applied to three selected localities, Motukarara, Rapaki Bay, and Hillsborough Valley to ascertain the warm spring's origin and source of heat. This thesis shows the Banks Peninsula warm springs to be an eastward extension of the metamorphic-hydrothermal system associated with the Alpine Fault. Water $\delta^{18}O$, δD, $\delta^{13}C$ and soil-gas $\delta^{13}C$ values are consistent with a metamorphic hydrothermal system dominated by meteoric water, similar to the Alpine fault hot-springs system. Analyses of the warm springs' gas and water isotopic and geochemical compositions reveal similar type waters to the Alpine Fault hydrothermal system that has mixed with local Canterbury Aquifer System (CAS) waters. Low temporal variance, combined with the elevated temperatures and localised nature of the Banks Peninsula warm springs suggests a strong structural control on the upper crust fluid flow of this system.

ACKNOWLEDGEMENTS

Firstly, I would like to thank my supervisors Travis Horton and Chris Oze, for their help in the field, suggestions, and brilliant advice which has only made this thesis better.

Matt Hanson, my soil-gas flux guru, without whom I would probably be staring at code in frustration. Thanks for the great times in the field, knowledge, and advice. Thanks also goes to all the kind people that allowed me onto their property to take samples, the wonderful locals of Banks Peninsula for contributing their knowledge of the warm springs, Max Borella for not only ending me his FLIR but also his phone, Melanie and Nicky for help in the field, Mitch Green for showing me his sites and data, my lovely office mates and colleagues on the fourth floor Von Haast, and the wonderful technicians and staff from both the University of Canterbury Geology and Chemistry departments for sharing their expertise, helping me with my samples, finding equipment, and showing general interest in my project and mental wellbeing; without you all this would have been a very different thesis

Finally, I would like to thank my family and friends for their endless encouragement, support, and understanding. None of this would have been possible without you.

TABLE OF CONTENTS

Frontispiece ii
Abstract iii
Acknowledgements iv
List of Tables v
List of Figures vi
1. Introduction 1
1.1 Thermal Springs in New Zealand 1
1.2 Banks Peninsula and its Warm Springs *2*
1.3 Contribution of this Thesis *3*
2. Objectives 5
3. Background and Review 6
3.1 Banks Peninsula's Geology and Geological History 6
3.1.1 Torlesse Supergroup (~230-20.5 Ma) 7
3.1.2 Lyttelton Volcanic Group (12.4-9.7 Ma) 7
3.1.3 Quaternary Sediments 8
3.2 Faulting in Banks Peninsula 8
3.2.1 The Canterbury Earthquake Sequence 10
3.3 Hydrology of Banks Peninsula 10
3.4 Warm Springs 11
3.4.1 Motukarara 11
3.4.2 Rapaki Bay 12
3.4.3 Hillsborough Valley 12
4. Methods 14
4.1 Sample Sites and Materials 14
4.2 Water Studies 15

4.2.1 Anion Analysis 16

4.2.2 Cation Analysis 17

4.2.3 Stable Isotopic Analysis 18

4.3 Soil-Gas Flux, Temperature, $\delta^{13}CCO_2$, and $\delta^{13}CCH_4$ Surveys 18

4.3.1 Sampling 20

4.3.3 Processing of Raw Data 22

5. Results 25

5.1 In field Observations *25*

5.1.1 Motukarara *25*

5.1.2 Rapaki Bay *26*

5.1.3 Hillsborough Valley 28

5.2 Water 28

5.2.1 Water type and chemistry 30

5.2.2 Water Isotopic Studies *39*

5.4 Gas 43

6. Discussion 47

6.1 Temporal Variation and Earthquake Inducement of the Banks Peninsula Warm Springs 47

6.2 Banks Peninsula, an Extension of the Alpine Fault Geothermal System 50

LIST OF TABLES

Table 2.1: Research Questions and Approach.....5

Table 5.1: Chemical analysis of Banks Peninsula Warm Springs.....35

Table 7.1: Research Questions and Answers 56

LIST OF FIGURES

Figure 1.1: Location of known geothermal springs within New Zealand with geothermal gradients modified from Reyes (2010) 1

Figure 3.1: 1:100,000 Scale geological map of Lyttelton Volcanic Group (LVG), Banks Peninsula, modified from Sewell et al. (1992).. 6

Figure 3.2: Simplified Geology of Banks Peninsula with known faults and sample locations modified from Ring and Hampton (2012). 9

Figure 3.3: Epicentres of earthquake and aftershocks related to the CES modified from Kaiser et al. (2012). 10

Figure 3.4: Locations of Banks Peninsula warm springs modified from Brown and Weeber (1994). 11

Figure 3.5: Looking south, the warm springs of Rapaki Bay below mid-tide, 22/1/2016. 12

Figure 4.1: Looking north, IR image identifying four of the five Rapaki Bay warm springs. 15

Figure 4.2: Sampling Alkalinity at site MS2.....16

Figure 4.3: Collecting soil-gas flux, $\delta^{13}C_{CO_2}$, and $\delta^{13}C_{CH_4}$ data at RBS1 with the IRGA-CRDS. 18

Figure 4.4: Setting up the survey grid at Rapaki Bay 20

Figure 4.5: IRGA-CRDS with generator, utilising a garden trolley for transportation at Rapaki Bay. 21

Figure 5.1: Motukarara warm springs. 255

Figure 5.2: changes in "soil" colouration of Rapaki Bay beach sand, near RBS4 26

Figure 5.3: Rapaki Bay warm springs. 277

Figure 5.4: Charge balance of Banks Peninsula warm spring sample sites. 29

Figure 5.5: Water chemistry of Banks Peninsula warm springs.....31

Figure 5.6: Cl^--SO_4^{2-}-HCO_3^{2-} ternary diagram (Giggenbach, 1988) for thermal water comparisons 32

Figure 5.7: Sodium:Chloride ratio for Banks Peninsula warm springs.....33

Figure 5.8: Bicarbonate as a function of Total Dissolved Solids (TDS).....33

Figure 5.9: $(Na^{+} + K^{+})/Ca^{2+}$ versus Cl^{-} (mg/L) of Banks Peninsula warm springs. 34

Figure 5.10: Anion versus Cl^{-} (mg/L) of Banks Peninsula warm spring samples. 36

Figure 5.11: Close up of Figure 5.10 non-ocean water contaminated samples.... 37

Figure 5.12: Cation versus Cl^{-} (mg/L) of Banks Peninsula warm spring samples. 38

Figure 5.13: Close up of Figure 5.12 non-ocean water contaminated samples.... 39

Figure 5.14: $\delta^{13}C$ (‰ V-PDV) versus $^{1}/_{DIC}$ indicating the heat source for the Banks Peninsula warm springs. 40

Figure 5.15: Isotopic bi-variant plot $\delta^{18}O$ versus δD for Banks Peninsula warm springs. 41

Figure 5.16: Close up of Figure 5.15 42

Figure 5.17: Temperature contour overlain on IR image of RBS2-4 43

Figure 5.18: Rapaki Bay temperature Survey. 44

Figure 5.19: Isotopic trends of Rapaki Bay soil-gas flux survey 45

Figure 5.20: CO_2 and CH_4 soil-gas emissions from Rapaki Bay warm springs. 46

Figure 6.1: Results from the combined temperature and soil-gas flux surveys at Rapaki Bay with inferred fault trace. 49

Figure 6.2: Cartoon of the proposed mechanism for Banks Peninsula warm springs. Image modified from (Cox et al., 2015).....51

Figure 6.3: Close up of Figure 5.7 53

1. INTRODUCTION

Crustal fluid flow is an important aspect of modern earth systems. The influence crustal fluids have on rock deformation and rheology as the result of water-rock interaction via fluid transport at elevated pressure and temperature is an important problem facing modern geoscience.

Geothermal systems provide globally significant resources that can be economically valuable in the case of hydrothermally associated precious mineral deposits, and environmentally responsible in terms of providing a source for low-carbon energy. Being able to determine the origin of crustal fluids, their flow paths, through to their surface discharge conditions is crucial for understanding the interaction between rocks, water, and their associated volatiles. This thesis explores upper-crustal fluid flow of an anomalous and understudied low-enthalpy warm spring system situated at Banks Peninsula, New Zealand; one of the world's most active origins.

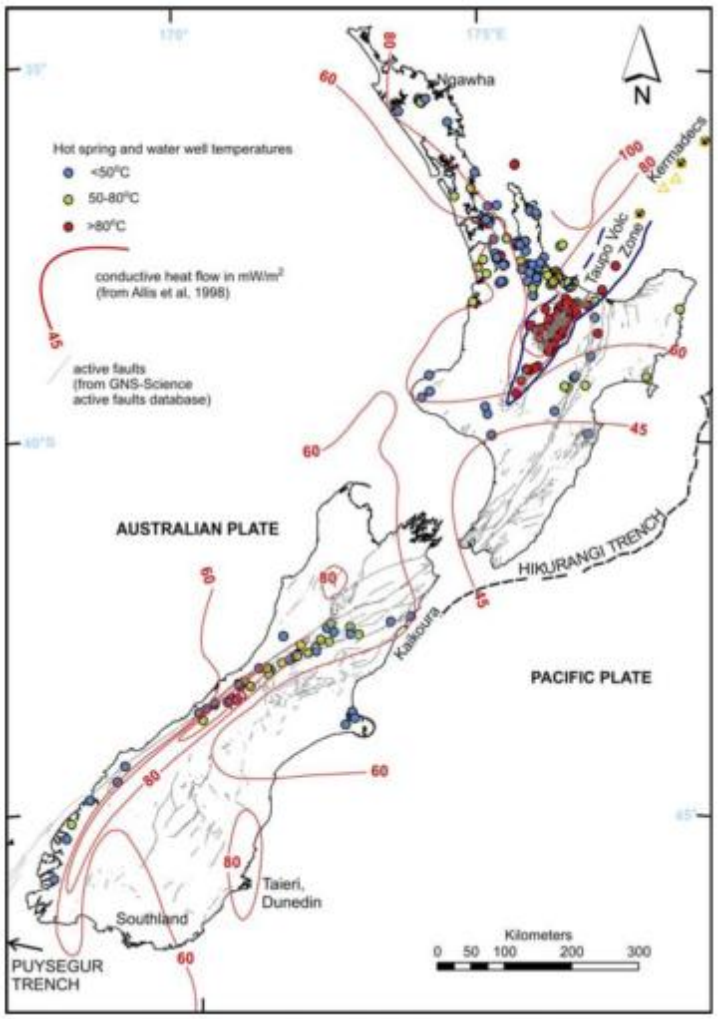

Figure 1.1: Location of known geothermal springs within New Zealand with geothermal gradients modified from Reyes (2010). Banks Peninsula, the location for this study (red circle) sits below the 60°C contour.

1.1 Thermal Springs in New Zealand

Thermal springs are "springs of naturally heated water" (*Oxford Dictionary*); of which there are ~140 of these identified within New Zealand (Reyes, 2010). These thermal springs are classified

as either: 1) hot springs systems with discharge waters <90°C, such as the Banks Peninsula warm springs 2) 120-160°C waters at >3.5 km in abandoned hydrocarbon wells, 3) natural heat flow found >15 m below the surface along fault conduits, and 4) high enthalpy geothermal system peripheries. The majority of these springs are located in the North Island, primarily within the Taupo Volcanic Zone (TVZ). Only 8% of New Zealands thermal springs reside within the South Island, including the warm springs of Banks Peninsula (Figure 1.1; Reyes and Jongens, 2005). The majority of these South Island thermal springs are associated with the Alpine and Hope Faults (Reyes, 2010) and account for 70% of the recognised South Island mineral spring systems.

1.2 Banks Peninsula and its Warm Springs

Banks Peninsula or *Te Rakaihautu* is the remnant of an extinct Mid-Late Miocene volcanic complex and is the largest Cenozoic intraplate volcanic province in the South Island (Figure 1.1; Sewell et al., 1992a; Sewell et al., 1993; Hoke et al., 2000; Reyes and Jongens, 2005; Forsyth et al., 2008; Hampton and Cole, 2009; Timm et al., 2009; Ring and Hampton, 2012). The mechanism behind the Miocene aged volcanics on Banks Peninsula has been an area of much debate; with lithospheric detachment being the current leading hypothesis for the volcanic complex's formation (Reyes and Jongens, 2005; Hoernle et al., 2006; Timm et al., 2009; Hampton, 2010; Timm et al., 2010).

In 1884, Laing reported the discovery of warm springs at Banks Peninsula (Brown and Weeber; 1994). Since Laings initial report, study of the springs has been sporadic with most studies focussing on the springs potential as a water resource for the Peninsula's local communities, their role as part of the extinct volcanic system, dating of the volcanics, or as part of the national geothermal resource (Sanders, 1986; Dorsey, 1988; Brown and Weeber, 1994; Reyes and Jongens, 2005; Reyes and Britten, 2007; Timm et al., 2009; Reyes, 2010; Reyes et al., 2010; Timm et al., 2010). The most recent study on the area was completed by Reyes et al. (2010), who

looked at the springs as part of a national overview of the countries low-temperature mineral spring systems.

The warm springs reside within the north-west composite Lyttelton shield volcano, the oldest in Banks Peninsula's volcanic complex (Sewell et al., 1992a; Brown and Weeber, 1994; Forsyth et al., 2008; Hampton and Cole, 2009; Timm et al., 2009; Ring and Hampton, 2012). Despite the volcanic surrounds of the warm springs the seismic tomography study completed by Montelli et al. (2006), revealing no magmatic thermal anomaly beneath the volcanic province, removes any qualm of a fresh volcanic heat source for the warm springs. This lack of a magmatic anomaly, in conjunction with minimal observed gas, and the restriction of the warm springs to the oldest volcanic group of the volcanic complex suggests that the heat source for the warm springs is not likely to be volcanic in origin (Reyes and Jongens, 2005; Timm et al., 2009).

The most recent study by Reyes et al. (2010), reported the Banks Peninsula warm springs to be the result of meteoric fluids that had been heated at depth. Structural control, especially inherent faulting, has significantly impacted the formation and placement of the Lyttelton Volcanic Group (LVG; Hampton, 2010). Restriction of the warm springs to such a structurally controlled geologic unit coupled with the springs' alignment along some of the more inherent basement faults; suggests a more structural related origin to the warm spring fluids. The hypothesis of a potential structural relationship between faulting and the warm springs is further evidenced by the occurrence of new warm springs; along with the reported increase in activity of pre-existing warm springs in relation to the 2011 Canterbury Earthquake Sequence (CES).

1.3 Contribution of this Thesis

This thesis presents the first soil-gas flux survey of the Banks Peninsula hydrothermal system. The CO_2 released from the hydrothermal system can be used as a proxy for total mass and heat transfer (Bloomberg et al., 2014; Hanson et al., 2014a), providing a complimentary data set to to the more traditional aqueous studies for interpretation. The addition of both water, $CO_{2\,(g)}$, and

$CH_{4\,(g)}$ carbon istopes to previously observed oxygen and hydrogen isotopes for the new and pre-existing warm springs, will enable a better picture of the debated heat source of the Banks Peninsula hydrothermal system to be formed (Giggenbach, 1992). The heat source of the elevated temperatures (~4-20°C above 'background' levels) observed at the warm springs is a major gap in the understanding of the Banks Peninsula hydrothermal system. This heat source has been postulated to arise from either local meteoric water interacting with deep thermal gradients beneath the peninsula, or from direct interaction with the volcanics (Brown and Weeber, 1994; Reyes et al., 2010) however, the elevated temperatures of the warm springs may represent indirect magmatic influence through rock weathering processes.

Despite the area being well studied (Sewell et al., 1992a; Forsyth et al., 2008; Hampton and Cole, 2009; Ring and Hampton, 2012), the source and structural control of the warm springs remains uncertain, making the Banks Peninsula warm springs one of the least understood geothermal systems in the country. This thesis investigates both the fluids and gases evolved from the old and new warm springs of Banks Peninsula, in order to assess/confirm their origins as well as to determine their potential relationship with faulting.

2. OBJECTIVES

The two main objectives of this thesis are to: 1) determine the chemical origin of the Banks Peninsula warm springs through isotopic aqueous geochemical analyses, 2) quantify CO_2 and CH_4 gas fluxes originating from the Banks Peninsula warm springs to determine their heat source. Achieving these objectives will enhance New Zealand's understanding of its current geothermal resources their potential for development.

Table 2.1: Research Questions and Approach.

Question	Approach
What is influencing the elevated temperatures of the warm springs?	• Detailed soil-gas surveys surrounding the springs using an accumulation chamber linked to both IRGA (LiCOR) and CDRS (Picarro) • Comparison of CO_2 and CH_4 flux as a proxy with water DIC samples
What is the origin of the Banks Peninsula warm spring water?	• Stable isotopic analysis of δH, and $\delta^{18}O$ from water samples as a proxy for meteoric influence • Comparison and isotopic analysis of alkalinity ($HCO_{3(aq)}^-$) through and $CO_{2(g)}$ as a proxy for DIC • Comparison of sodium and chloride ratios from water samples to determine marine interference using IC and ICP-MS analysis

3. BACKGROUND AND REVIEW

3.1 Banks Peninsula's Geology and Geological History

Bedrock lithologies of Banks Peninsula are well known (Figure 3.1; Dorsey, 1988; Sewell et al., 1992a; Reyes and Jongens, 2005; Forsyth et al., 2008b; Timm et al., 2009; Ring and Hampton, 2012), comprising of the eroded remnants of four Mid to Late Miocene volcanic groups which overlay Rakaia Terrane greywacke basement (Mortimer, 2004; Forsyth et al., 2008). The smaller and intervening Mount Herbert (9.7-8.0 Ma) and later Diamond Harbour Volcanics (8.1-5.8 Ma) are eclipsed by the north-east Lyttelton (11-9.7 Ma) and south-west Akaroa (9.1-8.0 Ma) composite shield volcanoes, all of which overlay

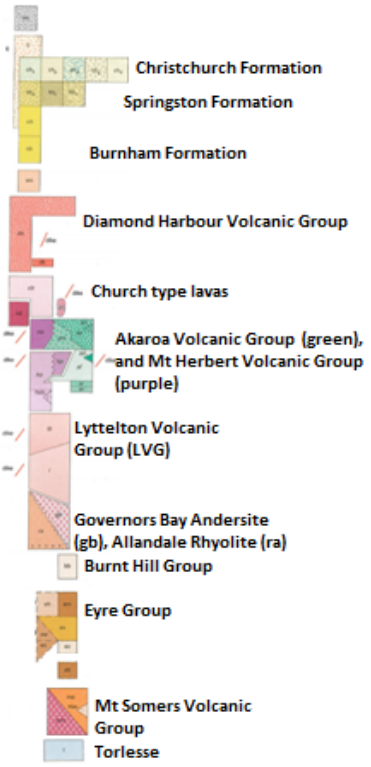

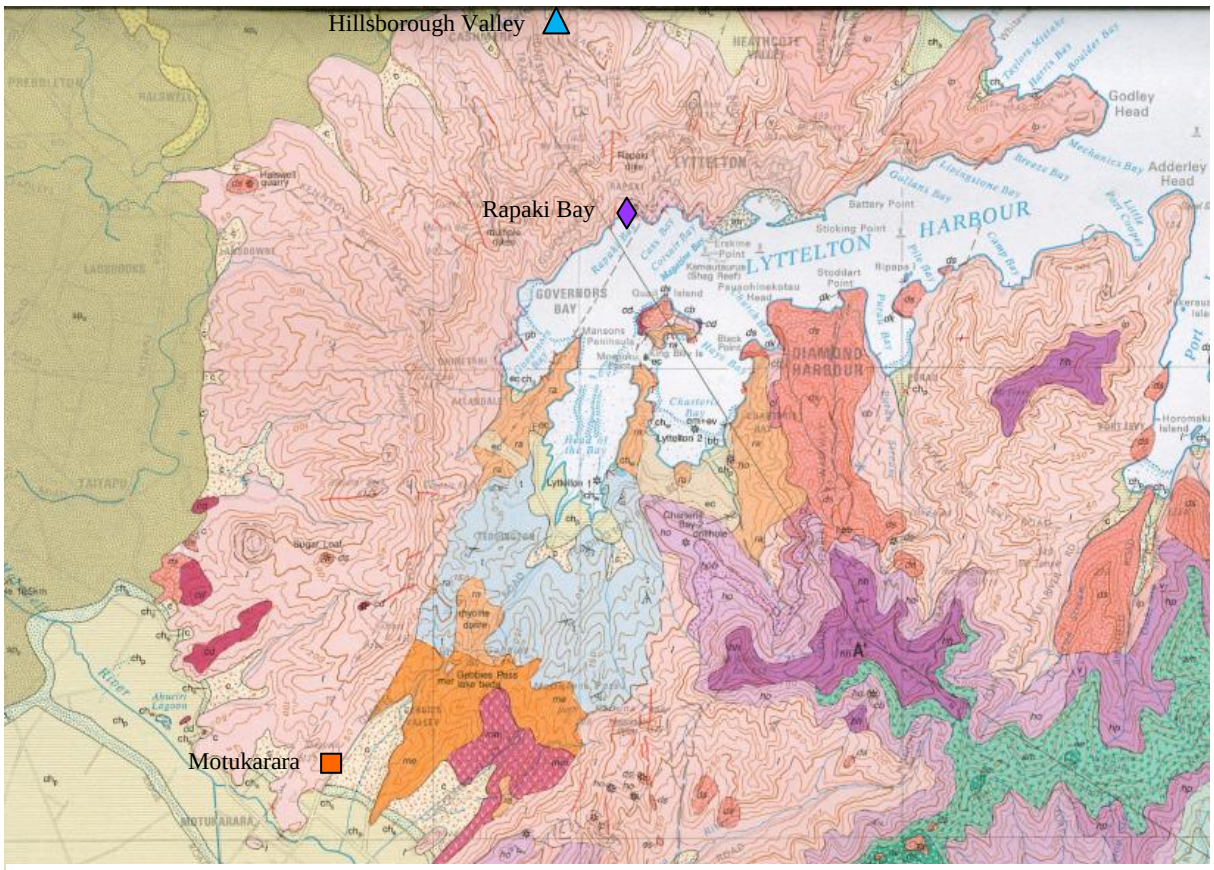

Figure 3.1: 1:100,000 Scale geological map of Lyttelton Volcanic Group (LVG), Banks Peninsula, modified from Sewell et al. (1992a). All of the Banks Peninsula warm springs lie within the LVG, including the sampled springs from this thesis.

the older Mt Somers Volcanics (Sewell et al., 1992a; Reyes and Jongens, 2005; Forsyth et al., 2008; Timm et al., 2009; Ring and Hampton, 2012). Bedrock faults provide permeable conduits for water flow throughout heavily eroded and highly desiccated volcanics, with some basement being visible valleys such as Gebbies Pass (Sewell et al., 1992a; Forsyth et al., 2008).

3.1.1 Torlesse Supergroup (~230-20.5 Ma)

The Torlesse Supergroup is the oldest formation found in the Canterbury region (Sewell et al., 1992a; Mortimer, 2004; Forsyth et al., 2008). Deformed, slightly metamorphosed, and consisting of sedimentary argillite and greywacke it forms the basement rock of Banks Peninsula. Exposed in Gebbies Pass the basement rock is comprised of quartz, low albite, chlorite, calcite, laumonite, and muscovite (Barnes et al., 1978). Evidence from drillholes and deep wells around the Canterbury region suggests that the torlesse acts as conduit for groundwater, housing the aquifers of the Canterbury Aquifer System (CAS) in its highly fractured crush-zones (Taylor et al., 1989; Brown and Weeber, 1994; Reyes, 2010).

3.1.2 Lyttelton Volcanic Group (12.4-9.7 Ma)

Active between 12.4-9.7 Ma (Forsyth et al., 2008; Ring and Hampton, 2012), the Lyttelton Volcanic Group (LVG) encompasses the Lyttelton and Mount Pleasant Formations (Figure 3.1). The LVG is the only volcaninc group on the peninsula to host warm springs (Sewell et al., 1992a; Brown and Weeber, 1994). Consisting of sub-alkaline plagioclase-olivine-clinopyroxene phyric hawaiites, mugearite, and benmoreite basaltic to trachytic flows, interbedded with breccias, tuff, scoria lava domes, and cut by basaltic to trachytic dykes as well as plagioclase-clinopyroxene-olivine-orthopyroxene phyric andesitic flows; the volcanism of the LVG is considered to be controlled by underlying fault linearments (Altaye, 1989; Sewell et al., 1992a; Forsyth et al., 2008; Hampton and Cole, 2009; Ring and Hampton, 2012).

3.1.3 Quaternary Sediments

Extensive erosion is evident within Banks Peninsula, significant amounts of loess has been deposited on Banks Peninsula through aeolian transport processes during glacial periods. These deposits are seen to thicken towards the base of the Peninsula infilling drainage channels and eroded valleys. Classified into two types, Birdlings Flat and Barrys Bay, the loess is predominantly distinguished by locality rather than its chemical composition, due to redistribution of leached salts from rainfall events (Griffiths, 1973). Canterbury gravels also cover the lower portions of the volcanic complex's outer flanks, connecting the former island to the South Island via the Canterbury Plains (Sewell et al., 1992a; Forsyth et al., 2008; Hampton, 2010).

3.2 Faulting in Banks Peninsula

Faulting within the peninsula was initially inferred by Sewell et al. (1992), due to the linear placement of the warm springs within the LVG. These formerly inferred 'warm spring' faults are now recognised as sections of the Gebbies Pass Fault System (normal) and the Mt Herbert Fault (dextral strike-slip), two of the five fault systems present on the peninsula (Figure 3.1; Ring and Hampton, 2012). The Gebbies Pass Fault system is related to the Canterbury Horst first-order regional structure and has been considered, alongside other bedrock faults, as a possible conduit for water flow in the region (Brown and Weeber, 1994; Forsyth et al., 2008; Ring and Hampton, 2012). Structures such as the Gebbies Pass Fault system may play an important role in determining the source origin source of the Banks Peninsula warm springs (Sanders, 1986; Giggenbach, 1992; Brown and Weeber, 1994; Ring and Hampton, 2012).

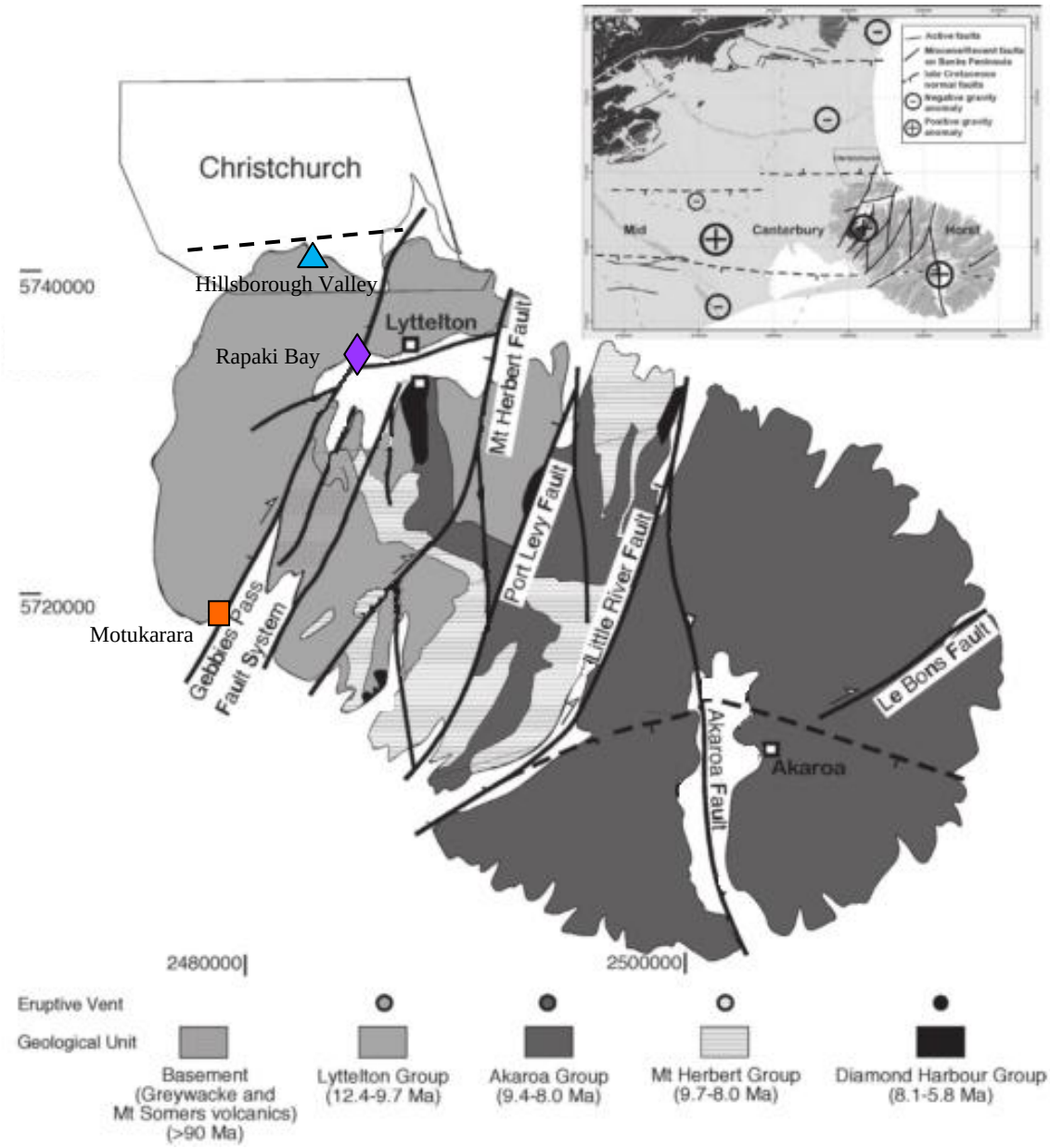

Figure 3.2: Simplified Geology of Banks Peninsula with known faults and sample locations, which lie along the faults. Inset shows the position of Banks Peninsula within the Canterbury tectonic regime. Image modified from Ring and Hampton (2012).

3.2.1 The Canterbury Earthquake Sequence

The 6.2 Mw earthquake on the 22nd February and associated pre-/aftershocks of the Canterbury Earthquake Sequence (CES) had a significant effect throughout the LVG (Figure 3.2;Bannister et al., 2011; Beavan et al., 2011; Kaiser et al., 2012; Ring and Hampton, 2012; van Ballegooy et al., 2013), resulting in increased gaseous activity and localised semi-linear expansion of active warm springs (Gorman, 2011), alongside the appearance of multiple new springs within the Hillsborough Valley, an area with no known history of springs prior to the event (Green, 2015)

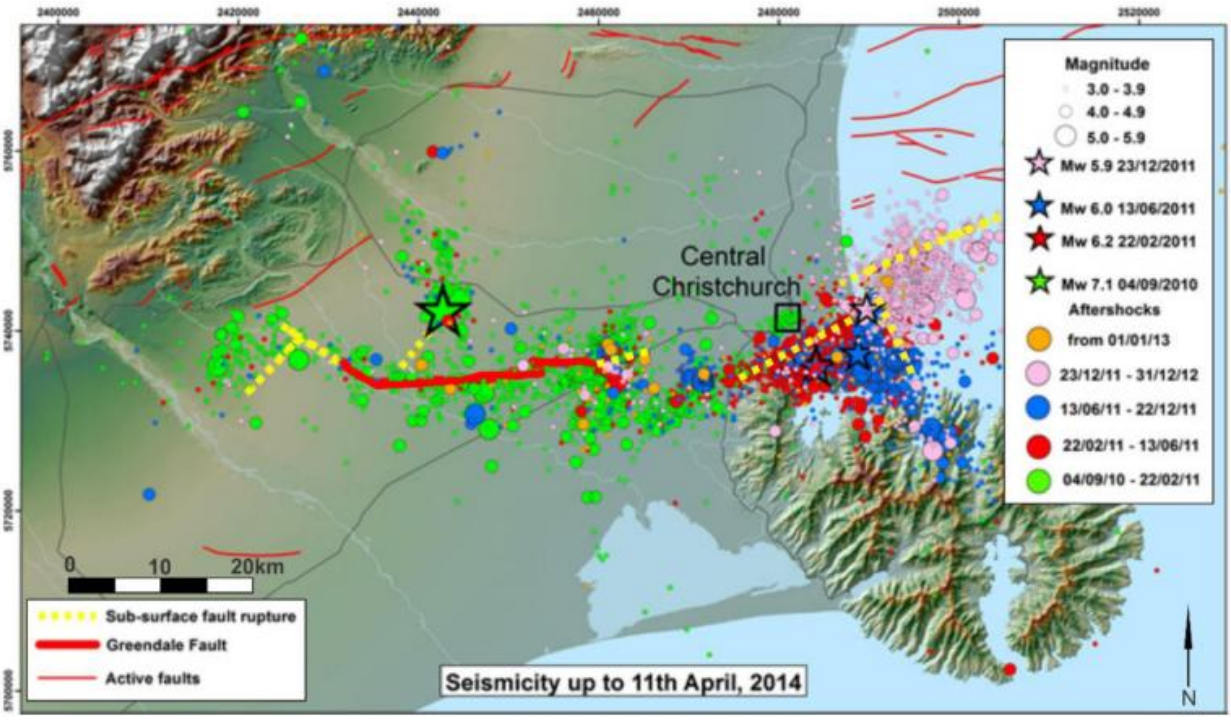

Figure 3.3: Epicentres of earthquake and aftershocks related to the CES modified from Kaiser et al. (2012). Aftershock activity from the CES is observed within the Rapaki Bay and Hillsborough Valley sampling regions from this thesis.

3.3 Hydrology of Banks Peninsula

There has been very little information published surrounding the hydrology of Banks Peninsula. Currently, the Peninsula is thought to receive its water supply primarily through meteoric recharge from local surface features such as shallow spring fed rivers, with the fractures present within the volcanic rock acting as the recharge sources (Christchurch City Council, 2009; Environment Canterbury, 2011).

3.4 Warm Springs

Internationally, there has been much debate regarding the classification of warm springs. To date there is no universally applied definition in terms of temperature range. For this study warm springs are classified as thermal waters that are <90°C as stipulated by (Reyes and Jongens, 2005) and at least 4°C above the average water temperature (Canterbury water ca. ~12-13°C; Stewart, 2012). Using this definition, 6 warm springs have been reported within Banks Peninsula, 4 of which were considered active prior to the CES (Figure 3.3; Sewell et al., 1992a; Brown and Weeber, 1994; Thain et al., 2006; Reyes et al., 2010).

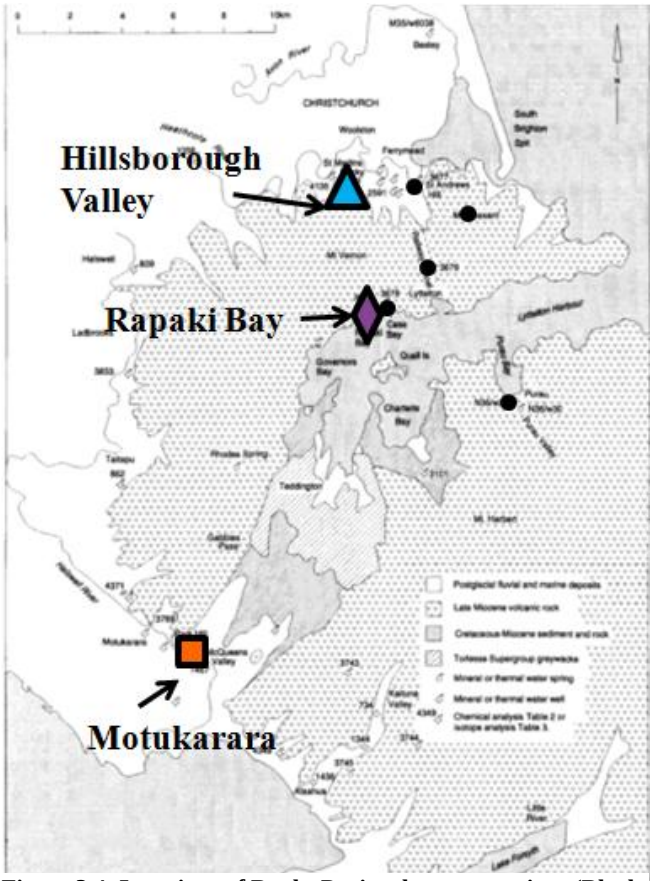

Figure 3.4: Locations of Banks Peninsula warm springs (Black dots) modified from Brown and Weeber (1994). Motukarara (orange square), Rapaki Bay (purple diamond), and new site Hillsborough Valley (blue triangle) indicate sites from this thesis.

3.4.1 Motukarara

Motukarara lies towards the outer-flanks of the LVG, along the eroded Gebbies Pass valley (Figure 3.5). Here, three warm springs were identified at a private Teddington Farmstead located at the base of a loess hill. The water from two of the springs (MS1 and MS2) is seen to emit out of the fractured olivine basaltic rock face as described by Brown and Weeber (1994), the confined nature of the bedrock preventing any soil-gas survey around the springs. No samples were collected for the third spring (MS2) due to its diffusivity and extremely low condition.

3.4.2 Rapaki Bay

Situated in the upper portion of Lyttelton Harbour, Rapaki Bay is the third embayment south of Lyttelton Port. Formed within the eroded andesitic volcanic rock, Rapaki Bay hosts the warmest of all the springs noted by Brown and Weeber (1994). Currently, there are five established intertidal springs located within the Bay which are used by the public for recreation and bathing. The largest and warmest of these are easily identified via stones in the sub-tidal beach face outlining the temporary bathing pits (Figure 3.5).

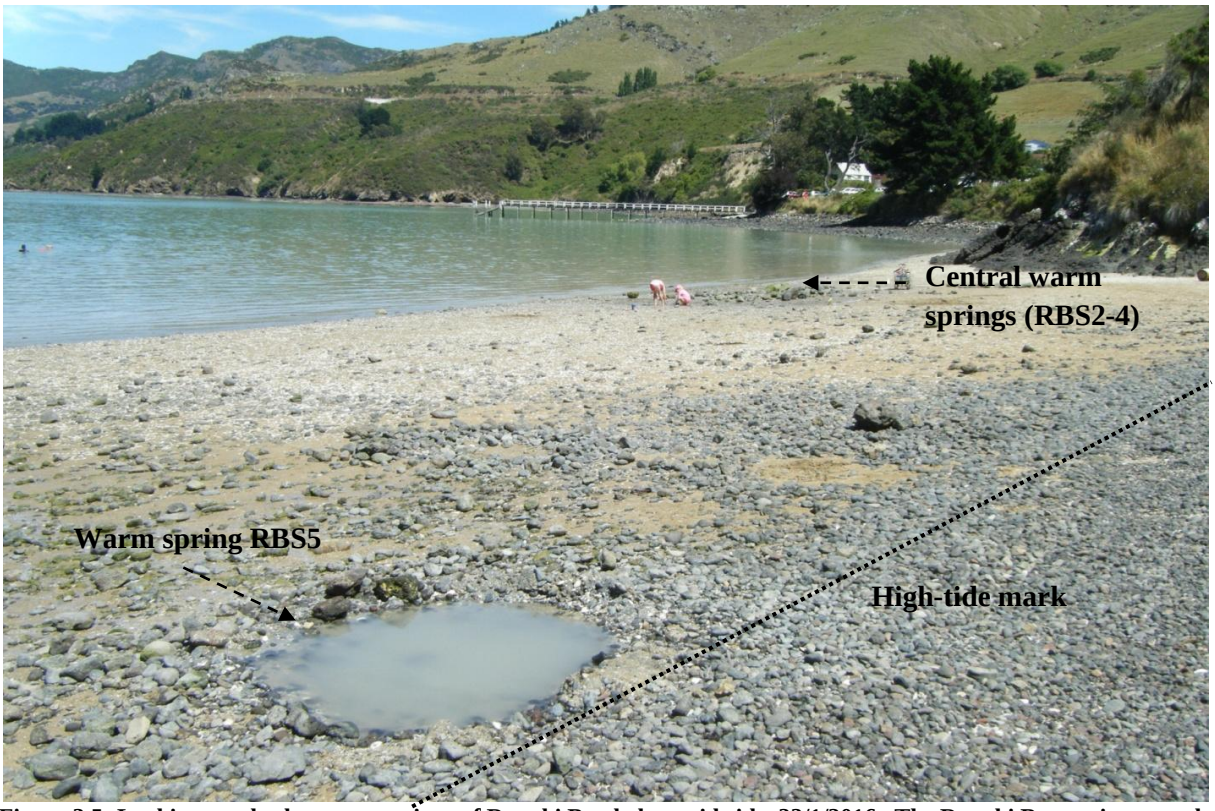

Figure 3.5: Looking south, the warm springs of Rapaki Bay below mid-tide, 22/1/2016. The Rapaki Bay springs are the only warm springs on the peninsula freely accessible to the public. Here the springs are pictured as remnants of bathing pits

3.4.3 Hillsborough Valley

Hillsborough Valley is situated in an infilled erosional valley on the outer flanks of Banks Peninsula, within the Heathcote river catchment. The lithology of the valley consists primarily of Birdlings Flat loess which underwent compaction and subsidence in relation to the CES (Griffiths, 1973). Coincident with earthquake induced compaction and subsidence of the valley, multiple springs appeared at the surface; most of which were noted to appear following the

February 22nd M_w 6.2 earthquake (Green, 2015). For this study, only two of these springs were selected for analysis (HVS1 and HVS2) based on their accessibility and suitability for sampling. Both springs exhibit discernible flow, are diffuse, and occur underneath residential buildings. Due to the nature and occurrence of these particular springs (HVS1 exits from under the house foundations and HVS2 has been redirected from underneath the house to pipes situated around the property) only water samples were able to be taken.

4 METHODS

4.1 Sample Sites and Materials

Three locations, Motukarara, Rapaki Bay, and Hillsborough Valley, were selected within the northeastern Lyttelton Volcanic complex of Banks Peninsula (Figure 3.3). These sites were chosen due to their "undisturbed" state ((Thain et al., 2006), in comparison to the warm springs noted by Brown and Weeber (1994) that have been modified, redirected, infilled or dried up. Two of these locations, Motukarara and Rapaki Bay, were studied over an extended period of time (ca. ~32 years) and have been anecdotally reported to have undergone expansion post the 2011 Canterbury Earthquake Sequence (CES) (Brown and Weeber, 1994; Thain et al., 2006; Reyes and Britten, 2007; Forsyth et al., 2008; Reyes, 2010; Reyes et al., 2010). The third site, Hillsborough Valley, hosts new springs which appeared as a consequence of the CES.

Five Springs were identified at Rapaki Bay, three springs at Motukarara, and two of the five monitored springs by Green (2015) were selected to be studied in Hillsborough Valley. GPS coordinates of the sampled springs were recorded using a Garmin GPSmap 62S GPS. Both water and soil temperature were measured using a Center 370 RDT thermometer (accuracy ± 0.1 °C).

Samples were collected over the autumn-winter period 2015 from March-July. Soil-gas surveys, with associated soil temperature surveys, were undertaken at the Rapaki Bay site during dry stable conditions to minimise atmospheric pressure effects, meteoric water, soil humidity, and wind interference. Due to the Rapaki Bay springs being intertidal there was little control over the 'soil' (i.e. beach sand) humidity. In order to maintain some consistency, each of the two soil-gas flux surveys (25/3/2015 and 22/1/2016) at Rapaki Bay were performed during one tidal cycle.

4.1.1 Infrared Imaging

Infrared (IR) images were used to identify the warm springs at two of the three locations (Motukarara and Rapaki Bay; Figure 1). IR imaging was not used at the Hillsborough Valley sites due to the source of the springs being obscured by infrastructure. The HVS2 site also had the added complication of redirected spring water due to land modification at the site. All of the IR images were taken using a FLIR ONE infrared camera attached to an Apple i-phone 5.

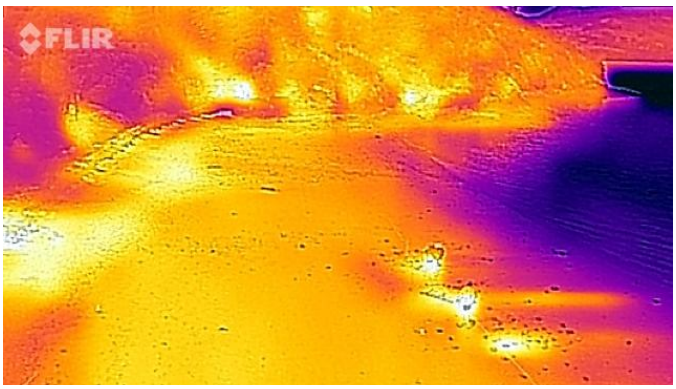

Figure 4.1: Looking north, IR image identifying four of the five Rapaki Bay warm springs.

4.2 Water studies

Individual water samples were collected in June 2015, reported isotopic samples from Rapaki Bay were collected March 2015 in conjunction with the initial soil-flux survey. The selected sample sites encompassed two of the three springs at Motukarara (MS1 and MS2), all five springs at Rapaki Bay (RBS1-5), and the two selected springs in Hillsborough Valley (HVS1 and HVS2). Additional ocean (RBO), meteoric (RBR), blank , and duplicate (RBS3D) water samples were taken at Rapaki Bay for comparison and quality control (Q_c). To avoid contamination of samples, fresh gloves were worn at each location and new syringes and filters were used for each spring sample collection.

All of the spring samples were taken at the point source of the spring (Figure 2), or in the case of the Hillsborough Valley samples, at the closest point with clear flow. All of the water samples, filtered and unfiltered, were collected via sterile Chirana 20 ml Luer syringes with the filtered samples using 0.45µL sterile Millex HA filter unit MF-millipore MCE membrane syringe filters. Collected samples were placed into new, rinsed with sample, 15 mL centrifuge tubes. The

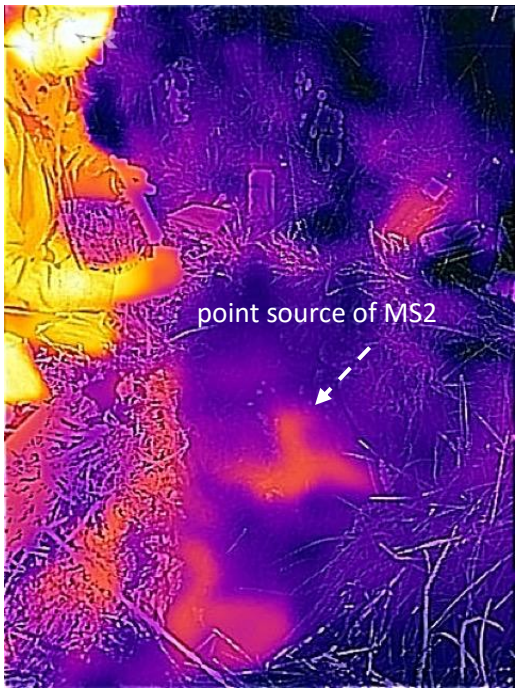

Figure 4.2: Sampling alkalinity at site MS2. The point source of the warm spring flows out of the fractured basaltic rock face just above ground level. The elevated temperature of the water is clearly visible when viewed in the infrared.

samples determined for isotopic analysis were overfilled, removing any headspace before being capped, in order to prevent isotopic fractionation. The samples for trace metal and base cation analysis were then acidified with 10 µL of 70% ultra-pure nitric acid in a clean room at the University of Canterbury, Chemistry Department. The acidification of samples enabled the solution to be compared against calibration standards as well as stabilises the metals within the solution. All samples were maintained at 4°C between collection and analysis.

Spring water pH and conductivity were measured in the field using a Mettler Toledo SevenGo Duo pro Ph/Ion/Cond with meter heads, Mettler Toledo Inlab® Expert Pro-ISM-IP67 pH 0-14, 0-100°C and Mettler Toledo Inlab® 738 ISM Conductivity NTC 30 kΩ 0.01-1000 mS/cm, 0-100°C. The pH meter was calibrated at each site using standard pH 4.01 and 7.00 buffer solutions, with recordings being made for both unfiltered and filtered samples. Conductivity measurements were made only using filtered samples.

4.2.1 Anion Analysis

A general base anion suit was performed on collected 0.45µm filtered water samples. The filtered samples were analysed using a reagent-free DIONEX RF-IC 2100 Ion Chromatograph (IC) at the University of Canterbury, SABRE Lab. The concentration of anion species was determined by comparing the results produced from the IC against six prepared calibration standards (0.1, 1.0, 5, 25, 50, 100 mg/L).

4.2.1.1 Total Alkalinity

Total alkalinity ($HCO_3^-{}_{(aq)}$) was measured in-field using the USGS approved method. 0.1 N H_2SO_4 $_{(aq)}$ was used in conjunction with the Mettler Toledo SevenGo Duo pro pH meter. Samples RBS1-5 and HVS1-2 were filtered using 0.45 μm Millex HA filter units with MF-millipore MCE membranes, MS1-2 were filtered using LabServ nylon membrane non sterile 25 mm 0.2 μm syringe filters. The data was processed using the USGS alkalinity calculator using both the Inflection Point and Gran methods for comparison (USGS, 2012; USGS, 2013).

4.2.2 Cation Analysis

K^+, Na^+, Al^{3+}, Mg^{2+} and Ca^{2+} were analysed using filtered and unfiltered samples using the Agilent 7500 Series Inductively Coupled Plasma Mass Spectrometer (ICP-MS) with Octopole Reaction System at the University of Canterbury, Chemistry Department. Unless otherwise stated; all the samples underwent 21x dilution in 10 ml 2% HNO_3 prior to analysis. The exception lies with the RBS3 and RBS4 samples which underwent 51x dilution in 10 ml 2% HNO_3 due to their elevated chloride concentrations, and the RBR and blank samples which were undiluted. The unfiltered and filtered blanks, taken in the field, were run alongside the duplicate (RBS3D) sample for quality control (Q_c).

4.2.2.1 Trace Metal Analysis

V, Cr, Mn, Fe, Co, Ni, Cu, Zn, As, Cd, Sb, and Pb were analysed using the same samples and methodology stated above for cation analysis.

4.2.3 Stable Isotopic Analysis

$\delta^{18}O$ and δD were analysed using a Picarro Liquid Isotope Analyser (LWIA) 1000 series at the University of Canterbury Stable Isotope Laboratory. For each sample, six lots of 2 μm fluid were injected into the LWIA, the first two injections were disregarded due to the memory effect. The mean and standard deviation were taken from the remaining four injections. $\delta^{18}O$ and δD were normalised against the VSMOW SLAP (Southern Latitude Antarctic Precipitation).

$\delta^{13}C$ and DIC was analysed using the Thermo Gas Bench II. Referenced against replicate analysis of NBS-19 and NBS-22 certified reference materials the stable carbon isotopic compositions are accurate to <0.10 ‰. $\delta^{13}C$ was normalised to VPDB.

4.3 Soil-Gas Flux, Temperature, $\delta^{13}CCO_2$, and $\delta^{13}CCH_4$ Surveys

Two soil-gas flux surveys were undertaken at Rapaki Bay, with associated temperature surveys. An initial survey was carried out late March 2015 and a more detailed survey Late January 2016 (Figure 4.4). The soil temperature was taken at 10 cm depth using a Centre 370 RDT thermometer, the initial 2015 survey incompassed RBS2-4 in a 12.5 x 30 m grid, with 1 m horizontal spacing and 2.5 m lateral spacing; following the same grid as the soil-gas flux survey. Additional point surveys were taken around each of the springs and other notable features in the later 2016 survey. Soil-gas flux measurements were taken using the accumulation methodology modified from Chiodini et al. (1998) by Hanson et al. (unpublished.b) using a combined West Systems LI-COR 820 infrared

Figure 4.3: Collecting soil-gas flux, $\delta^{13}CCO_2$ and $\delta^{13}CCH_4$ data at RBS1 with the IRGA-CRDS.

CO_2 gas analyser equipped with a WS-HC-IR $CH_{4\ (g)}$ detector, H_2S detector and 1,000 SCCM pump (henceforth IRGA) and a Picarro G2201-i CO_2 and CH_4 isotopic Cavity Ring Down Spectroscope with additional SSIM2 and modified re-circulating pump, (standard flow rate 25 SCCM; henceforth CRDS) henceforth referred to as IRGA-CRDS (Figure 4.3). The accumulation chamber used was an A type West Systems accumulation chamber with a cross sectional area of 3.140×10^{-2} m^2, an internal volume of 2.756×10^{-3} m^3 that contained an appropriate vent, butyl rubber septa for discrete sampling, and a mixing vane. The IRGA is calibrated annually with a sensitivity range of 0-20,000 ppm (CO_2) , a 10,000 ppm sensitivity range for CH_4; with a detection limit of 60 ppm, and has an H_2S sensitivity range of 0-25 ppm; with a detection limit of 0.02 ppm. Company precision of the flux is reported at 3%, but has been reported in the literature as ± 10 % for flux ranging 0.2-200 $gm^{-2}day^{-1}$ (Chiodini et al., 1998; Hanson et al., 2014b) and ± 5 % for fluxes greater than 200 $gm^{-2}day^{-1}$(Hanson et al., 2014b). The CRDS has a company guaranteed precision of <1 ‰ for concentrations up to 500 ppm; <0.5 ‰ for concentrations 500-1,500 ppm; and <0.2 ‰ for concentrations 1,500-3,000 ppm and a maximum detection limit of 7,000 ppm (~ 300 $gm^{-2}day^{-1}$ with the given size of the accumulation chamber) (Hanson et al., unpublished.b). CRDS fluxes are reported to be 102% of the traditional soil-gas flux meter values (Hanson et al., unpublished.b) The CRDS was calibrated daily via running 4 psi standard gas for 40 minutes prior to and post sampling. Running the standard gas not only enabled internal calibration of the device but also enabled the instrumental drift to be accounted for. In order to covert the flux from ppmv to $gm^{-2}day^{-2}$ air temperature (AT) and air pressure (AP) was required. The AT was provided on an hourly basis by the New Zealand MetService from the Lyttelton Harbour weather station situated ca. 2.5 Km from Rapaki Bay. The AP was extracted from the IRGA during data processing.

4.3.1 Sampling

A sampling grid was constructed following the collection of IR imagery encompassing all five Rapaki Bay warm springs (Figure 4.4). Initial measurements were taken using the IRGA to determine the presence of measureable flux. Measurements <0.1 ppm $CO_{2\,(g)}$ were deemed to be null flux sites based on the instruments measurement error. Positive flux sites were then re-assessed using the combined IRGA-CRDS. The IRGA-CRDS flux measurements were taken over a five minute period per flux site as per the methodology discussed in Hanson et al. (unpublished.b; Figure 4.3). The start and stop times of which were recorded manually for processing. The five minute period enables a decent amount of flux and to be accumulated within the chamber; from which an identifiable linear trend can be deduced, while maximising the amount of survey points that can be assessed throughout the sampling period, and enabling a reasonable amount of isotopic data to be collected by the CRDS for interpretation. Due to the lithology of loose medium to fine sand and the locality of the site; a modified shrub-tub was used as a secondary barrier (skirt) around the accumulation chamber to prevent wind interference. In order

Figure 4.4: Setting up the survey grid at Rapaki Bay: A) The initial survey late March 2015 B) Late January 2016.

to prevent contamination and enable more accurate flux data between each sample; the chamber was left to re-equilibrate/purge in the open air between consecutive measurements The time of re-equilibration was dependent on the concentration of the flux, with higher flux measurements requiring longer purge times

4.3.2 Infrared Gas Analyser-Cavity Ring Down Spectroscopy (IRGA-CRDS) Set Up

The accumulated chamber gas exits the outlet port via a 75 mL water trap, containing magnesium perchlorate ($Mg(ClO_4)_2$) $_{(s)}$, connected to a 0.45µm PFTE membrane filter. From there, the gas travels along 5 m of PFA tubing (ID: 4 mm, OD: 6 mm) to a 6 mm Swagelock T junction made from stainless steel. Here the gas is split into two pathways, one part travels through the IRGA and the other through $^1/_8$ tubing through a copper filled H_2S trap designed by Hanson et al. (unpublished.b) into the CRDS. The H_2S trap utilises a Costech water trap which is then packed with ~12 g of 0.7 mm diameter reduced copper wire and a small amount of quartz wool. Upon exiting the IRGA and CRDS analysers the two pathways are combined at another T junction prior to the gas being transported back into the accumulation chamber along another length PFA tubing. The IRGA was deployed in the field using a low emission petrol generator for power and was transported by a garden cart (Figure 4.5).

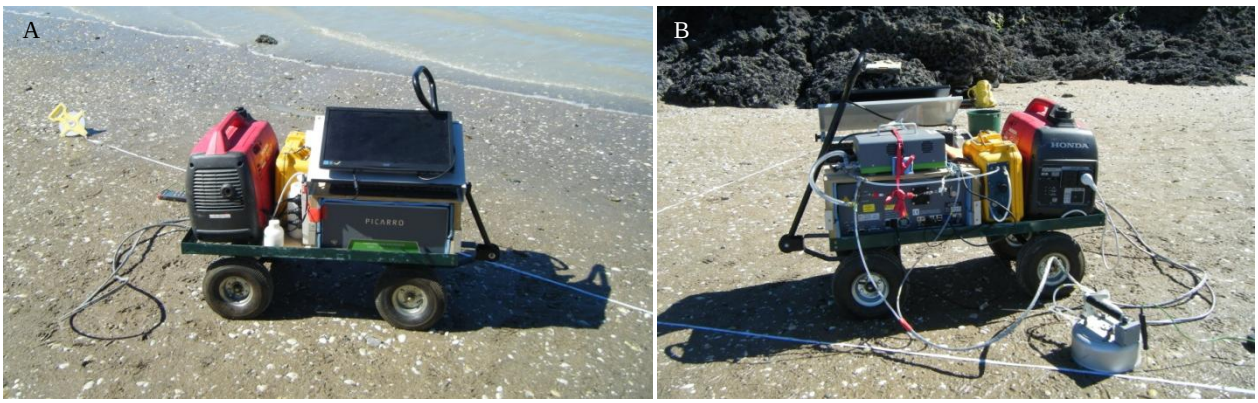

Figure 4.5: IRGA-CRDS with generator, utilising a garden trolley for transportation. A) The IRGA-CRDS in action at Rapaki Bay. Both analysers run independent of one another but analyse the same gas in real time. The generator and monitor are linked to the CRDS, the monitor is used to observe the incoming data and monitor the Chem detect trigger. The IRGA runs off its own batteries and is has its own handheld monitor. B) The IRGA-CRDS set up. Tubing circulates the incoming gas from the accumulation chamber through the IRGA (yellow case) –CRDS (grey case) analysers before returning the gas to the accumulation chamber.

4.3.3 Processing of Raw Data

Both the flux and isotopic data collected from the IRGA- CRDS was analysed using a code written for the Freeware R (Hanson et al., unpublished.b). The data was manually checked for wind interference and triggering of the CRDS interfering chemical detector. This enables Qa and Qc to be maintained prior to further processing of the data. The chemical detector is activated when any given species overloads the sensor within the CRDS, this can be due to an interfering gas species such as H_2S or high gas concentrations that exceed the device's detection limit. Both the flux and isotopic raw data we assessed in terms of linearity.

4.3.3.1 Flux Determination

The flux traces provided by the IRGA and CRDS were assessed separately, with each individual flux trace of each species undergoing separate analysis. The Flux traces are visually classified into one of three types: 1) linear, 2) semi-linear, and 3) non-linear. The non-linear fluxes were automatically discarded leaving only the linear-type traces. Type 2 flux traces were manually edited by either removing the initial or last few data points in order to form new type 1 plots which could then be analysed. Manually editing each of the individual flux traces is time consuming but enables representative subsets of the data to be retrieved from non-ideal flux traces such as those affected by wind interference, which would not have been able to be analysed if the flux traces were edited as a group. The linear traces are then assessed by either Linear Regression (LR) or Hierarchical Moderated Regression (HMR). Both methodologies are used in this thesis as currently there is no one internationally agreed method that can holistically and accurately represent the variation found within groups of collected flux data.

4.3.3.2 Stable Isotope Determination

The CRDS exploits the difference between carbon's ^{13}C and ^{12}C isomeric near-infrared absorption spectra, taking continuous isotopic measurements *in situ* with the soil-gas flux measurement to determine the gas's isotopic composition. The CRDS $\delta^{13}C$ measurements has an accuracy of ± 0.94 ‰ and -0.13 ‰, the precision of which is similar to the traditional Keeling plot methodology. In comparison to traditional IRMS techniques, the CRDS is less precise ± -0.2-1.0 ‰ and requires larger discrete samples (> 20 mL) and the use of a $H_2S_{(g)}$ trap to prevent interference of H_2S's near-infrared spectra with that of the ^{12}C ($CO_{2\ (g)}$) (Hanson et al., unpublished.b) but enables continuous analysis of both CO_2 and CH_4 $\delta^{13}C$ throughout the flux trace, creating and overall more representative isotopic signature for the survey area.

For the initial flux survey isotopic samples were taken in the traditional method to compare $\delta^{13}C_{CO_2}$ against the CRDS isotopic data and for quality control (Q_c). Soil-gas samples were collected in flushed $He_{(g)}$ 12 mL glass vials sealed with butyl septa lids. Gas samples were extracted via sterile syringe over seven seconds at the beginning and the end of each flux measurement as to not interfere with the IRGA-CRDS measurements. The extracted gas samples were analysed at the University of Canterbury, Stable Isotope Laboratory under continuous flow conditions using a Thermo Scientific GasBench II connected to a Delta V+ gas isotope ratio mass spectrometer, isotopic precision <0.16‰ $\delta^{13}C_{CO_2}$, <1.15, (accuracy <0.10‰ for repeated NBS-19 and NBS-22 certified reference materials)

The Keeling plot technique was used to calculate the isotopic composition from the raw CRDS isotopic data, plotting $\delta^{13}C_{CO_2}$ against the reciprocal $CO_{2\ (g)}$ concentration (i.e. $^1/_{[CO_2]}$) to create a linear model. This model was then visually evaluated for linearity via the flux plot, Keeling plot, normal Q-Q plot, residuals versus fitted plot, residuals versus leverage plot, and a scale versus location plot as described by Hanson et al. (unpublished.b). The coefficient of

determination (R^2) was not utilised due to its dependence on the Keeling plot y-intercept (isotopic composition of gas efflux).

5 RESULTS

5.1 In Field Observations

The warm springs from Banks Peninsula addressed in this study all occur in slightly different environments. The Motukarara springs discharge from volcanic bedrock on a working farm, the Rapaki Bay springs occur between the high and low tide mark discharging through the beach sand on an inlet within the Lyttelton Harbour, and the Hillsborough Valley springs all occur on residential property.

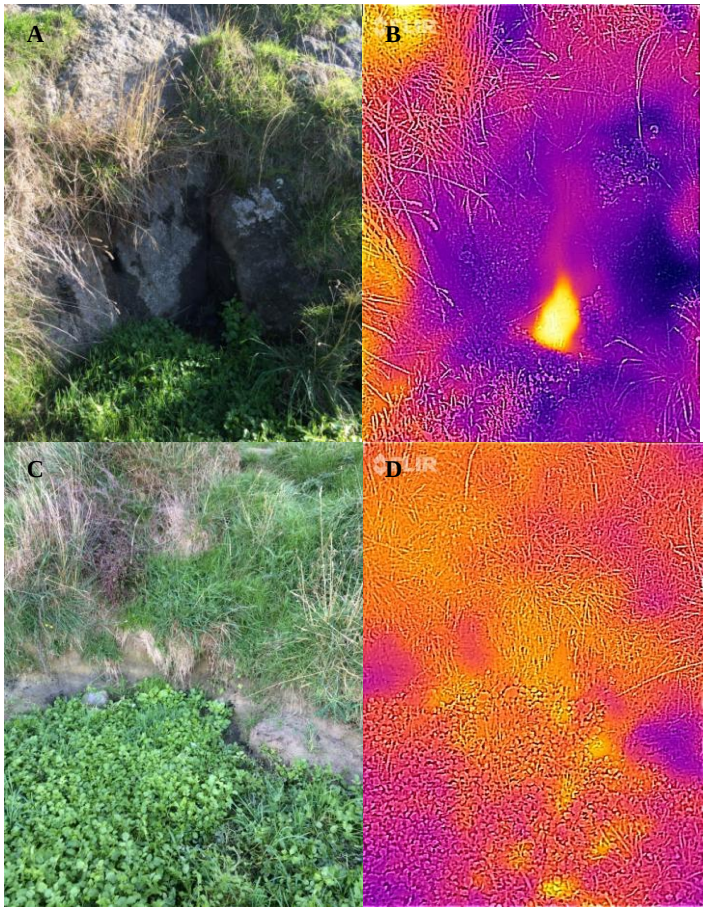

Figure 5.1: Motukarara warm springs; A) MS1 the highest temperature spring, water is flowing from basaltic rock, B) IR view of MS1 clearly identifying the point source of the water, C) MS3 (not sampled) the least active spring, D) IR image of MS3 the water is seen to be leaching from the loess from multiple places but no point source was identifiable.

5.1.1 Motukarara

Three warm springs are located at a Teddington Farmstead, northwest of Motukarara within 500 m from Gebbies Pass Rd (MS1, MS2, MS3) (Figure 5.1). The area consisits of walls of volcanic rock covered or overlain by a thick loess cover and thick mat of vegetation. The formation the "swampy bog" at the site , as described by Brown and Weeber (1994), results from lack of significant drainage coupled with the springs low flow rate.

Two of the springs (MS1 and MS2) discharge directly out of the dark grey fractured olivine basalt near the base of the wall, the third spring (MS3) discharges slowly and diffusely through the loess cover. MS1, the northern-most spring, is situated on a bouldery outjut and has two identifiable discharge points

(MS1 and MS1b, Figure 5.1). The discharge point on the south side of the outcrop has the highest flow rate and the highest temperature of all three springs (Table 5.1). MS2 discharges at ground level. The impedence of drainage from the surrounding vegetation has resulted in the water covering the point of discharge. MS3 has the lowest flow rate of all three springs, and as such very little can be discerned about the springs discharge point.

5.1.2 Rapaki Bay

Five warms springs are located at Rapaki Bay. The inlet within Lyttelton Harbour is surrounded by highly weathered and fractured andesitic rock which is intruded by dykes on the northeastern side. The springs are intertidal spreading from the high tide mark (RBS5) through to the low tide mark (RBS1) with the more developed central springs (RBS2-4) occuring in a linear line just below the mid-tide mark. Water discharging from the springs is observed coming through the sand as small restricted pockets of bubbling water. Gas associated with the heated water can be seen rising through the water column even when the springs are submerged, especially from the more developed springs (RBS2-4). The outflow of water runs oceanwards from the springs leaving a trail of cooling water, which is prominant in the IR images (Figures 5.3C, and 5.12). When the sand is dug up a colour change from brown to blue-black is noted 5cm below the surface (Figure 5.2) consistent with Brown and Weeber's (1994) observation. The blue-black change is apparent across the entire beach, but is more prominent nearer to the warm springs. The colouring is

Figure 5.2: changes in "soil" colouration of Rapaki Bay beach sand, near RBS4

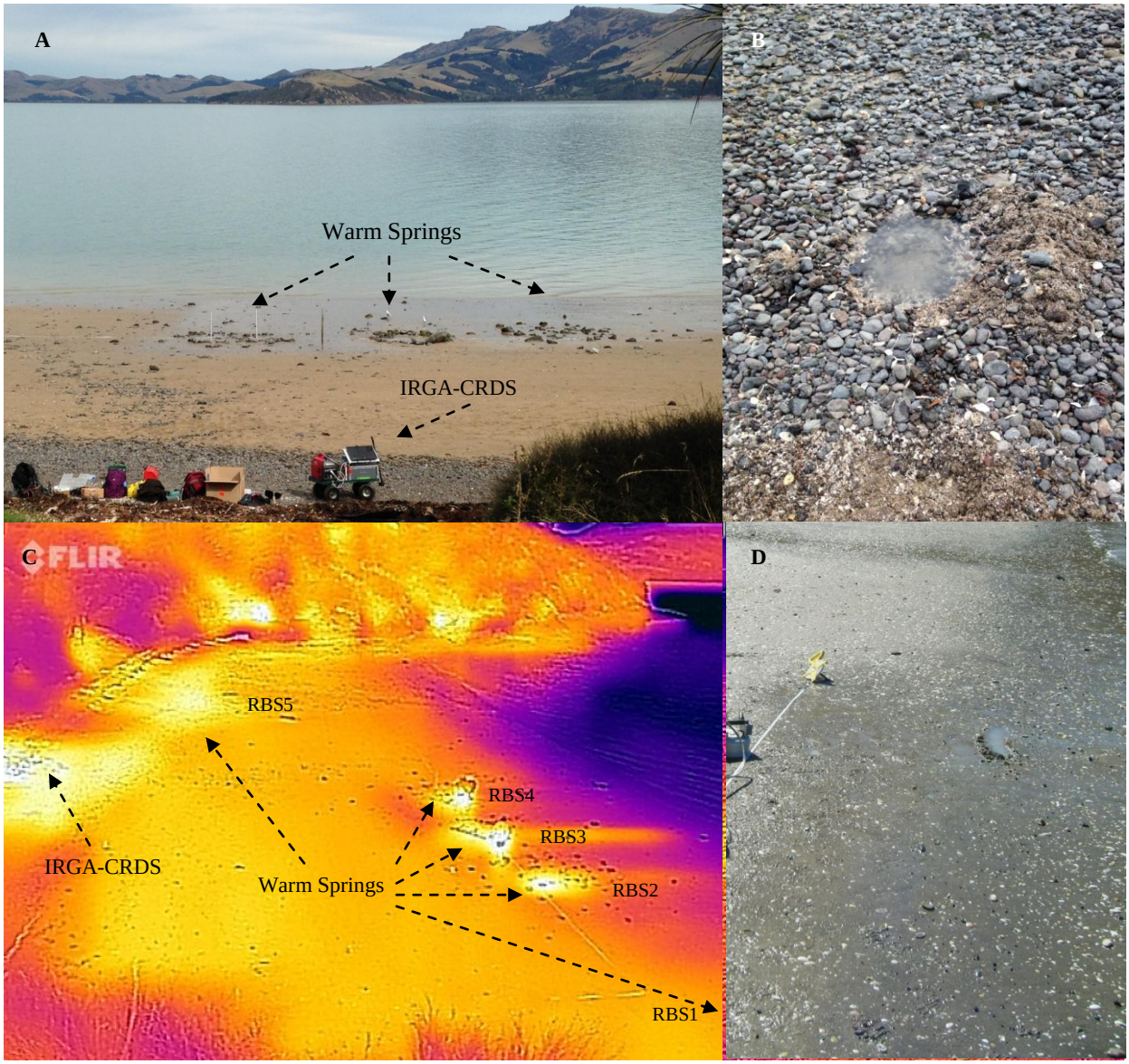

Figure 5.3: **Rapaki Bay warm springs A) Setting up the temperature and flux grid. Central warm springs are outlined with stones from remnant bathing pits. B) RBS5 one of the newer Rapaki Bay warm springs located at the high tide mark. C) IR image of the Rapaki Bay warm springs; RBS2-5 (pictured), and RBS1 (D), which is located just out of frame in the directionof the arrow D) RBS1, one of the newer springs, located < 1 m above the low tide mark.**

particularly apparent around RBS1, one of the least developed, and newer springs. A faint smell of hydrogen sulphide (H_2S) is also associated with the warm spring. (Figure 5.3D)

The temperature of the springs was measured in March and July. In Autumn RBS3 was the warmest of the five springs. However, when the samples were remeasured at the beginning of winter RBS2 and RBS5 had the warmest temperatures (Table 5.1). The lower temperature of

RBS3 is assumed to result from retained ocean water associated with the recently dug bathing pit which encompassed the warm springs at the time of sampling

5.1.3 Hillsborough Valley

There are multiple springs scattered throughout the Hillsborough valley region, diffuse discharge is the dominant type. The Hillsborough Valley is predominantly comprised of silty Birdlings Flat loess material, which underwent compaction and subsidence as a result of the Canterbury Earthquake sequence. The springs located in the area were non-existent prior to the quakes, with local residence reporting their occurance approximately 24 hours after the initial event (Green, *Personal Communication).* Water samples were taken at two different localities (HVS1 and HVS2), chosen for their accesibility and viability for sampling.

Two springs were initially present along a fissure trace underneath the residence at the HVS2 site (Green, 2015). The fissure was a direct result of ground movement associated with the CES. Prior to this thesis, the water from the two springs were redirected into three drainpipes located around the property. Only one of the three drainpipes were sampled in this thesis due to no water being present in the other pipes at the time of sampling.

Unlike the Motukarara and Rapaki Bay sites where the springs are closely related to the surrounding Lyttelton Volcanics, the BH-VRN-07 borehole taken at the HVS1 property revealed 48.4 m of Birdlings flat loess between the ground surface and the basalt of the Lyttelton Volcanic Group (*Tonkin & Taylor Report 52010.040*, 2011).

5.2 Water

The Spring waters range in p.H. from 7.5 in Motukarara to 8.4 in Rapaki Bay (Table 5.1).

Temperatures from 14.5°C in Hillsborough Valley to 33.6°C in Rapaki Bay (Table 5.1). Note that the Hillsborough Valley samples were not taken from the point source due to impeding

infrastructure, resulting in possible lower temperatures. Ionic charge matches that of previous studies (Figure 5.4), with Rapaki Bay exhibiting higher charge values. RBS3, the most active of the Rapaki Bay springs shows a species concentration double that of the other Rapaki Bay warm springs. This increased concentration is the result of remnant ocean water present in the spring at the time of sampling from a recently dug bathing pit encompassing the spring (Figures 5.3A and 5.12). Note that this ocean water contamination is not observed in the rapaki isotopic samples due to the isotopic samples being gathered at an earlier stage when the springs were in an untampered state. A similar level of ionic species concentration is seen in both the Motukarara and Hillsborough Valley samples. The difference in species concentration between the three locations may result from the locality of the springs and the amount of groundwater interaction present within the samples, with both Motukarara and Hillsborough Valley residing on the outer flanks of the Lyttelton Volcanic complex versus the Rapaki Bay springs which appears within its interior flanks, or the increased distance from the source.

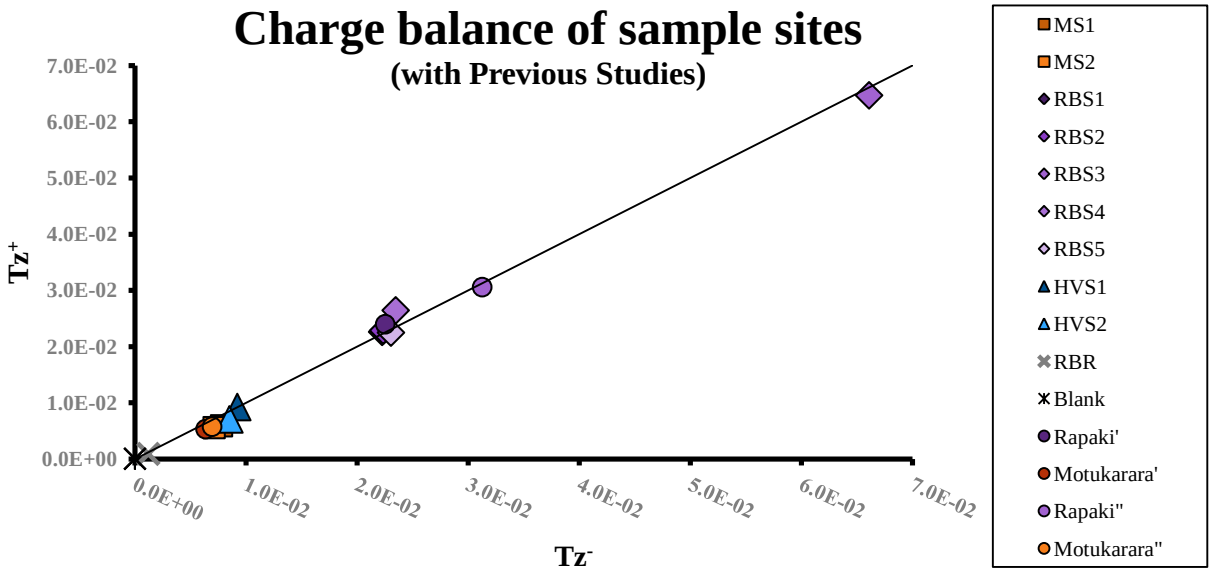

Figure 5.4: Charge balance of sample sites, Hillsborough Valley (blue), Motukarara (orange), and Rapaki Bay (Purple) with local rain (grey) Tz^+ (total cation charge) versus Tz^- (total anion charge). Additional data from Brown and Weeber, (1994)' and Reyes et al. (2010)". Collected samples from this thesis lie within a similar range to previous studies with the exception of RBS3. The observed higher concentration of charged species within RBS3 is the result of residual ocean water present within the sample.

5.2.1 Water Type and Chemistry

The Water for The Hillsborough Valley Springs plots within the realm of Na/Cl waters, similar to RBR and other Banks Peninsula warm springs sampled by Brown and Weeber (1994). This is chemically distinct from the Na/HCO_3 waters of the Motukarara and Rapaki Bay springs as well as the local groundwater (Ca/HCO_3) and local rain ($Na/Cl/HCO_3$) (Figure 5.5). However, when looking at the concentrations of the individual anions and cations; the Hillsborough Valley samples are similar those of the Motukarara springs (Figures 5.10-14). The major distinction between the two locations is lower bicarbonate (HCO_3^{2-}) and higher nitrate (NO_3^-) and chloride (Cl^-) concentrations within the Hillsborough Valley samples, that is indicative of the areas lithology and land use. Birdlings Flat loess is known for its low HCO_3^{2-} and high salt concentrations due to accumulation of the Barrys Bay leachate from weathering events (Griffiths, 1973).

The Banks Peninsula warm springs exhibit no signs of volcanic water. When plotted on a $Cl\text{-}HCO_3\text{-}SO_4$ ternary the waters plot within the peripheral water realm (Figure 5.6). The water trends from peripheral waters towards the mature waters, with the Hillsborough Valley samples exhibiting a more mature water signature, alongside RBS3 and RBS4 as a result of their higher chloride (Cl^-) concentrations.

RBS3 exhibits significantly higher chloride (Cl^-), bromide (Br^-), and sulphate (SO_4^{2-}) concentrations that plot within a similar region to a salt water contaminated CAS well reported by Hayward (2002) as well as higher sodium (Na^+) and potassium (K^+) concentrations (Figures 5.11 and 5.13) indicating salt water contamination from residual ocean water infilling the recently dug bathing pit that surrounded the spring. RBS4 also exhibits higher Br^-, and SO_4^{2-} levels and moderately higher magnesium (Mg^{2+}) and Na^{2+} levels than the RBS1, RBS2, and RBS3 samples that could also indicate trace amounts of reminant ocean water within the spring as an artifact from a previouly dug bathing pit (Figures 5.7-9, 5.10 and 5.12). RBS1, RBS2, and RBS5 samples exhibit no evidence of salt water contamination.

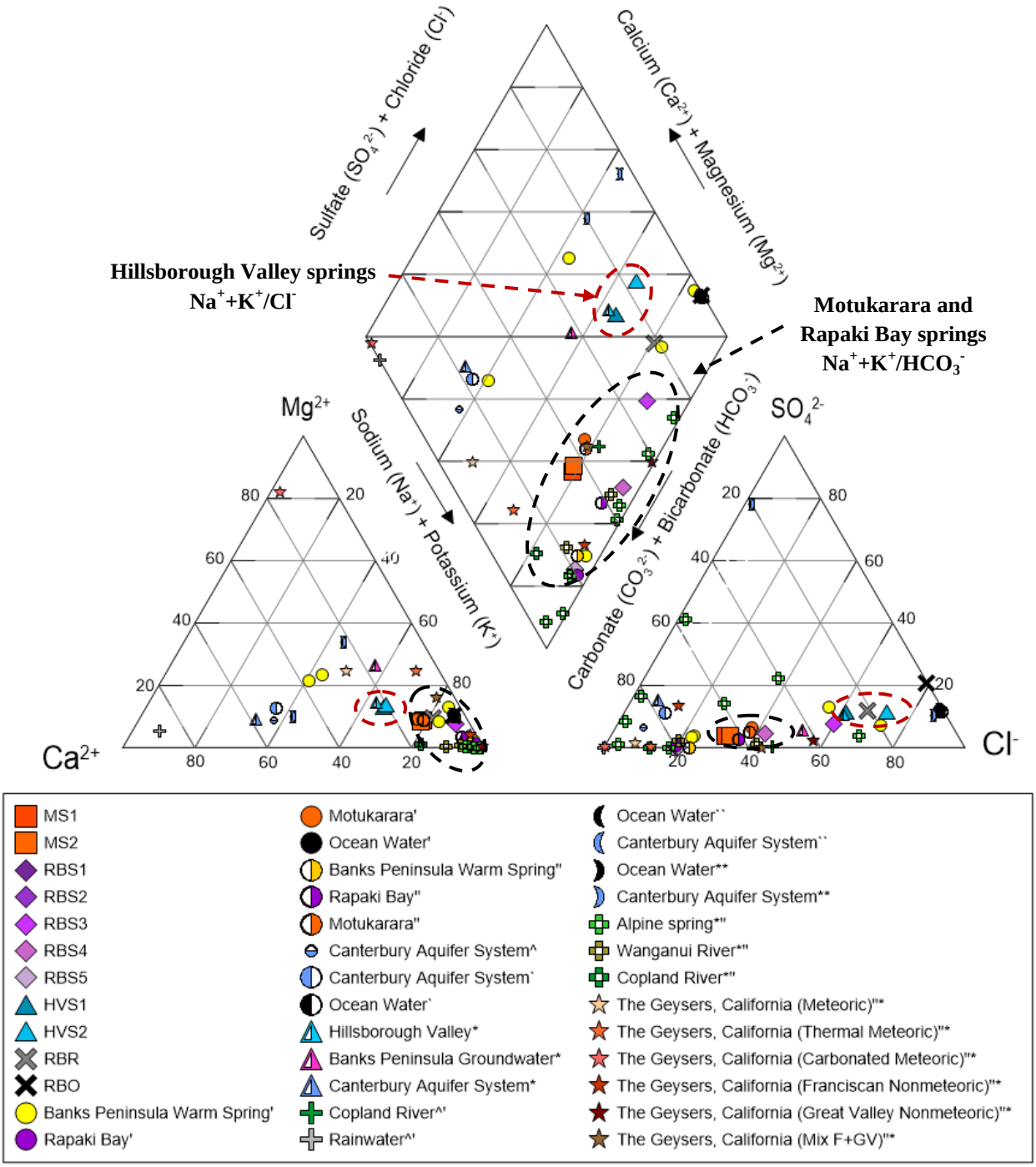

Figure 5.5: Water chemistry of Banks Peninsula warm springs. The springs chemistry is chemically distinct from both rainwater (RBR) and ocean water (RBO) samples (grey and black X respectively). Two dominant type are distinguishable Na^++K^+/HCO_3^- (black oval) and Na^++K^+/Cl^- (red oval) indicated above. Majority of the warm spring samples (Alpine Fault and Banks Peninsula) lie within the Na^++K^+/HCO_3^- group; the exception being the Hillsborough Valley samples. This is a result of excess chloride leaching from the surrounding Birdlings flat loess, a high salt concentrated loess (Griffiths, 1973). **Data presented in this diagram from previous studies are depicted using the following symbols: Brown and Weeber (1994)', Reyes et al. (2010)", Scott (2014)^, Aitchison-Earl et al. (2003)`,** Green, 2015***, Cox et al. (2015)^', Hayward (2002)``, Stewart (2012)**, Barnes et al. (1978)*", Donnelly-Nolan et al. (1993)"*.**

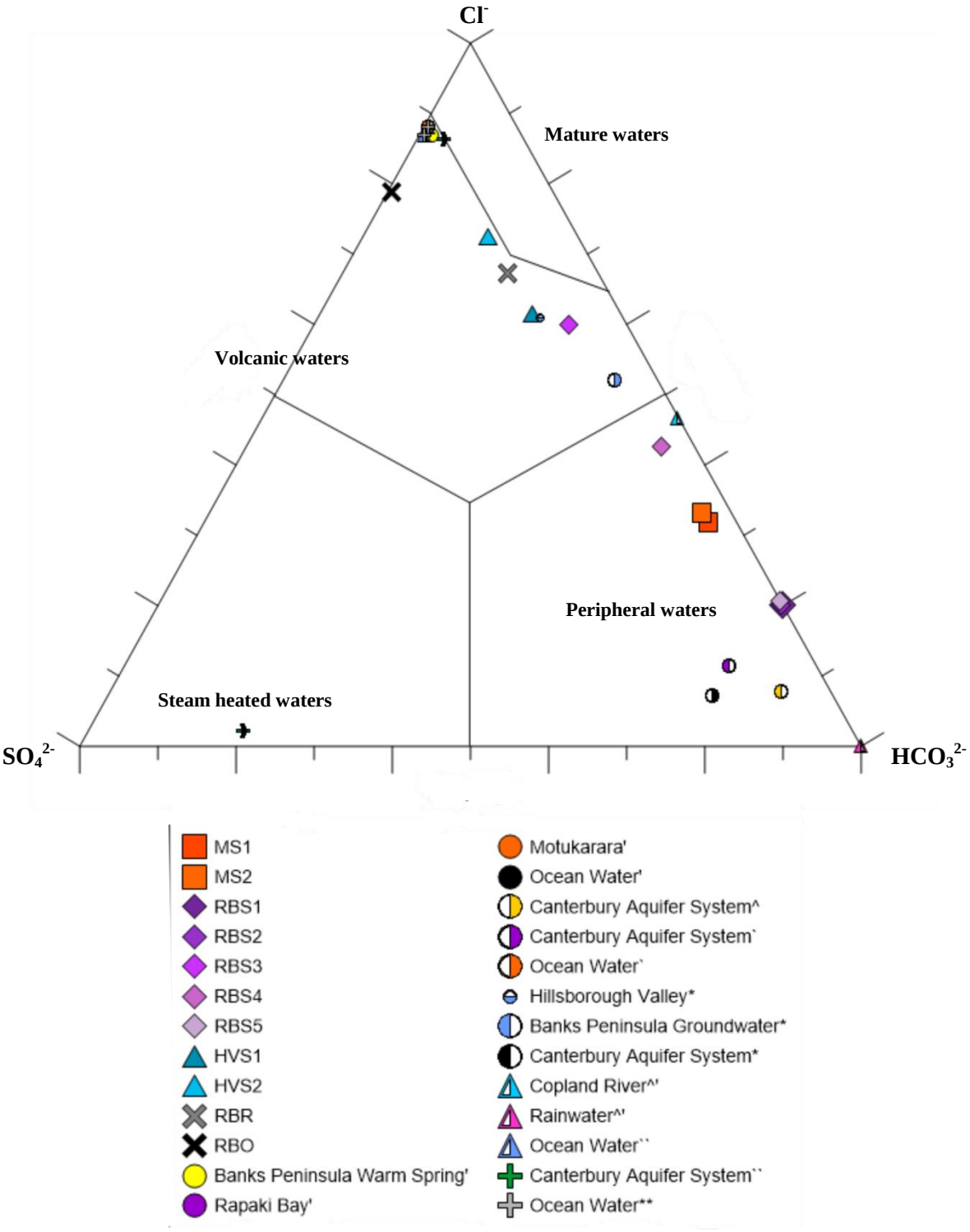

Figure 5.6: Cl^- –SO_4^{2-} –HCO_3^{2-} ternary diagram (Giggenbach, 1988) for thermal water compositions. The Banks Peninsula warm springs plot within the peripheral water, exhibiting no signs of volcanic influence. Additional data from Brown and Weeber (1994), Hayward (2002), Aitchison-Earl et al. (2003), Environment Canterbury (2014), and Cox et al. (2015).

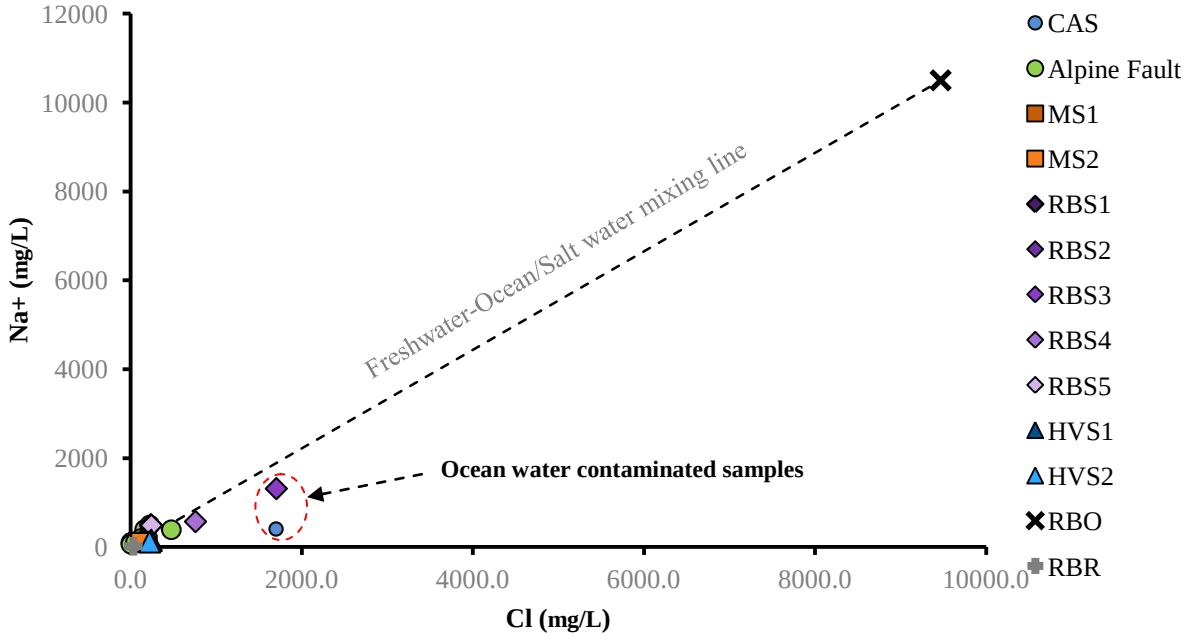

Figure 5.7: Sodium:Chloride ratio for Banks Peninsula warm springs, Alpine Fault springs (green circles), and Canterbury Aquifer System (CAS; blue circles). Samples sit along the freshwater-ocean water mixing line. Two of the samples exhibit same salt water influence; RBS3 and a known contaminated well from the CAS, marked in red.

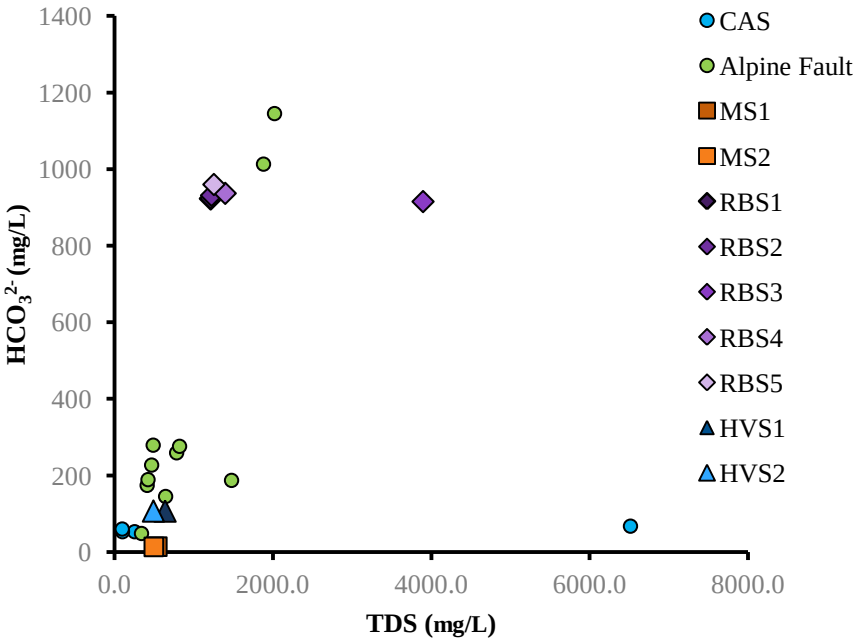

Figure 5.8: Bicarbonate as a function of total dissolved solids (TDS). Samples with high TDS exhibit signs of mixing with ocean water.

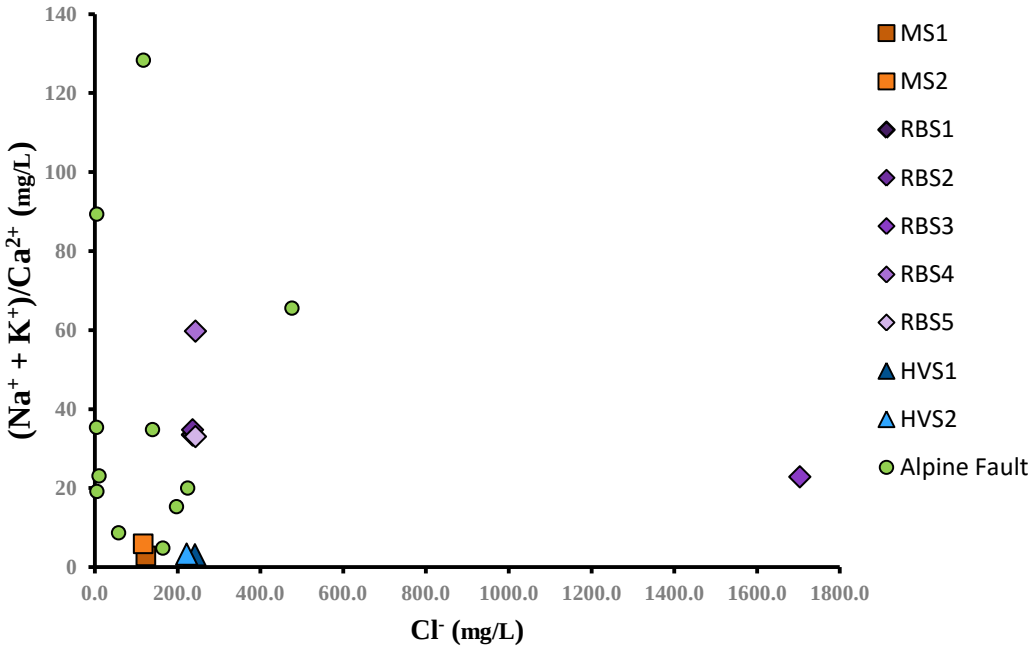

Figure 5.9: $(Na^+ + K^+)/Ca^{2+}$ versus Cl^- of Banks Peninsula warm springs. The Banks Peninsula samples, excluding RBS3, exhibit similar trends to Alpine Fault waters (additional data sourced from Barnes et al., 1978).

The rainwater sample (RBR) collected at Rapaki Bay also shows evidence of salt water contamination via sea breeze. Collected 100 m behind the beach in a grass clearing, RBR represents local rain from the Banks Peninsula area, exhibiting higher Arsenic (As), Cl^-, and Na^+ values typically associated with ocean water. Local signage from the Christchurch City council positioned ~95 m away from the raincatcher may have also influenced the copper (Cu) and chromium (Cr) concentrations present in the sample (Table 5.1).

All of the Banks Penisula warm springs exhibit high Na^+, Cl^-, and HCO_3^{2-} values 116-1703, 104- 1313, and 106-959 ppm respectively similar to Alpine Fault spring waters (Table 5.1, Figures 5.11 and 5.13). Linear trends can be drawn between the Motukarara and Rapaki Bay fluoride (F^-), Cl^-, phosphate (PO_4^{2-}), HCO_3^{2-}, Na^+, and K^+ samples, and between Motukarara and Hillsborough Valley samples for NO_3^-, Cl^-, SO_4^{2-}, Mg^{2+}, and Ca^{2+} samples. The uncontamianted Rapaki Bay samples tend to exhibit higher concentrations of dissolved species compared to the Motukarara and Hillsborough Valley samples, with the exception of $Mg^{2+}_{(aq)}$, $Al^{3+}_{(aq)}$, Ca^{2+}, and $NO_3^-{}_{(aq)}$ where the Hillsborough Valley samples are higher.

Table 5.1: Chemical analysis of Banks Peninsula warm springs

Locality		Motukarara		Rapaki Bay					Hillsborough Valley		Rain Water	Ocean Water	Blank
Sample		MS1	MS2	RBS1	RBS2	RBS3	RBS4	RBS5	HVS1	HVS2	RBR	RBO	Blank
Grid reference		43°43'22.58"S	43°31'22.43"S	43°36'27.26"S	43°36'27.30"S	43°36'27.34"S	43°36'27.42"S	43°36'27.34"S	43°33'57.92"S	43°33'44.34"S	43°36'27.20"S		-
		172°35'42.38"E	172°35'42.51"E	172°41'1.34"E	172°41'2.36"E	172°41'2.60"E	172°41'2.85"E	172°41'4.34"E	172°39'41.59"E	172°39'17.51"E	172°41'4.76"E		-
Temperature	°C	18.0	17.0	30.4	33.6	28.6	30.2	32.0	14.5	18.3	6.0	7.7	6.0
pH		7.5	7.7	8.4	8.2	8.2	8.2	8.2	7.7	7.5	6.9	8.1	-
Conductivity	µS/cm	678.030	650.050	1170.870	1168.830	7549.030	3441.610	1199.310	1193.800	1106.640	281.980	41312.810	-
Total Alkalinity	mg/L	249.300	221.100	922.900	931.300	915.200	936.700	959.800	106.600	107.000	10.000	49.200	<0.000
F	mg/L	0.156	0.144	2.898	3.001	2.577	2.945	2.945	0.236	0.229	0.122	0.304	0.001
Cl	mg/L	122.947	116.512	236.300	235.832	1703.376	242.842	242.842	241.575	221.527	31.855	9468.946	0.008
Br	mg/L	0.293	0.278	0.442	0.652	5.125	0.669	0.669	0.562	0.375	<0.000	40.585	0.030
NO3	mg/L	0.476	0.209	<0.000	<0.000	0.074	<0.000	<0.000	5.100	3.010	0.446	59.942	0.026
SO4	mg/L	13.984	13.366	0.349	1.870	214.267	77.570	1.400	44.868	35.243	5.557	2491.199	0.001
PO3	mg/L	3.864	3.102	4.352	4.635	5.275	5.525	6.672	3.041	3.472	5.741	6.434	0.001
Na	mg/L	111.390	104.871	489.880	494.879	1313.340	571.540	487.182	151.617	114.993	16.571	N.D.	0.030
Mg	mg/L	12.599	11.391	9.609	9.970	116.917	18.184	9.305	30.762	25.004	2.061	N.D.	0.001
Al	mg/L	0.009	0.016	0.019	0.031	0.037	0.029	0.014	0.015	0.010	0.103	N.D.	0.001
K	mg/L	2.841	2.638	19.997	20.374	49.368	22.059	20.011	4.455	3.516	0.845	N.D.	0.005
Ca	mg/L	17.821	18.205	15.210	14.818	59.606	9.936	15.343	49.861	35.871	1.967	N.D.	0.033
V	µg/L	18.527	18.159	0.721	3.080	3.462	1.019	0.135	3.008	8.619	0.353	N.D.	0.011
Cr	µg/L	<0.000	0.005	0.264	<0.000	0.403	<0.000	<0.000	0.401	0.444	4.505	N.D.	0.030
Mn	µg/L	<0.000	<0.000	70.666	89.514	85.88	49.601	10.843	1.643	14.538	11.533	N.D.	<0.000
Fe	µg/L	17.208	13.962	177.782	110.505	245.531	159.032	225.082	39.587	97.000	95.032	N.D.	0.302
Co	µg/L	<0.000	<0.000	0.001	0.060	0.006	0.044	<0.000	0.003	<0.000	0.305	N.D.	<0.000
Ni	µg/L	<0.000	<0.000	<0.000	0.022	<0.000	<0.000	<0.000	0.070	<0.00	1.708	N.D.	0.022
Cu	µg/L	0.36	0.183	0.486	0.400	0.359	0.475	0.438	0.253	0.016	15.497	N.D.	0.356
Zn	µg/L	5.643	14.492	8.621	4.078	23.034	8.594	3.533	4.100	4.214	421.578	N.D.	1.286
As	µg/L	0.574	0.665	3.635	6.609	8.267	3.084	1.81	1.347	1.264	2.284	N.D.	0.02
Cd	µg/L	0.042	0.02	0.016	0.053	0.138	0.012	0.021	0.064	0.058	1.695	N.D.	0.009
Sb	µg/L	0.797	0.686	0.462	0.401	0.908	3.340	0.399	1.797	1.082	0.764	N.D.	0.045
Pb	µg/L	0.104	0.036	0.069	0.189	0.399	0.131	0.053	0.249	0.056	1.444	N.D.	0.017
Na:Cl		4:3	4:3	3:1	3:1	1:1	7:2	3:1	1:1	4:5	4:5	-	
C	mMol/L	4.086	3.624	3.566	2.843	3.101	3.427	3.602	1.747	1.754	0.164	3.974	N.D.
1/DIC		0.245	0.276	0.280	0.352	0.322	0.292	0.278	0.572	0.570	6.101	0.252	N.D.
δ13C	‰ V-PDB	-13.35 ± 0.02	-13.52 ± 0.26	-6.32 ± 0.12	-6.13 ± 0.11	-6.15 ± 0.08	-6.03 ± 0.10	-6.23 ± 0.09	-15.56 ± 0.11	-14.82 ± 0.02	-8.62 ± 0.02	-1.22 ± 0.06	N.D.
DIC δ18O	‰ V-PDB	-11.42 ± 0.31	-11.46 ± 0.23	-12.90 ± 0.13	-12.75 ± 0.17	-12.71 ± 0.09	-12.35 ± 0.12	-13.13 ± 0.06	-10.36 ± 0.45	-11.39 ± 0.16	-10.92 ± 0.00	-5.58 ± 0.13	N.D.
H2O δ18O	‰ V-SMOW	-8.44 ± 0.13	-8.40 ± 0.05	-9.46 ± 0.07	-9.26 ± 0.17	-8.86 ± 0.10	-8.98 ± 0.17	-9.26 ± 0.06	-8.63 ± 0.06	-8.30 ± 0.08	-6.95 ± 0.06	N.D.	N.D.
δD	‰ V-SMOW	-61.35 ± 0.30	-61.85 ± 0.03	-64.04 ± 0.91	-64.19 ± 0.96	-60.15 ± 0.31	-62.14 ± 0.64	-62.97 ± 0.24	-61.95 ± 0.18	-62.14 ± 0.29	-42.85 ± 0.45	N.D.	N.D.
d excess		6.19	5.33	11.60	9.88	10.74	9.67	11.10	7.08	4.27	12.76	N.D.	N.D.

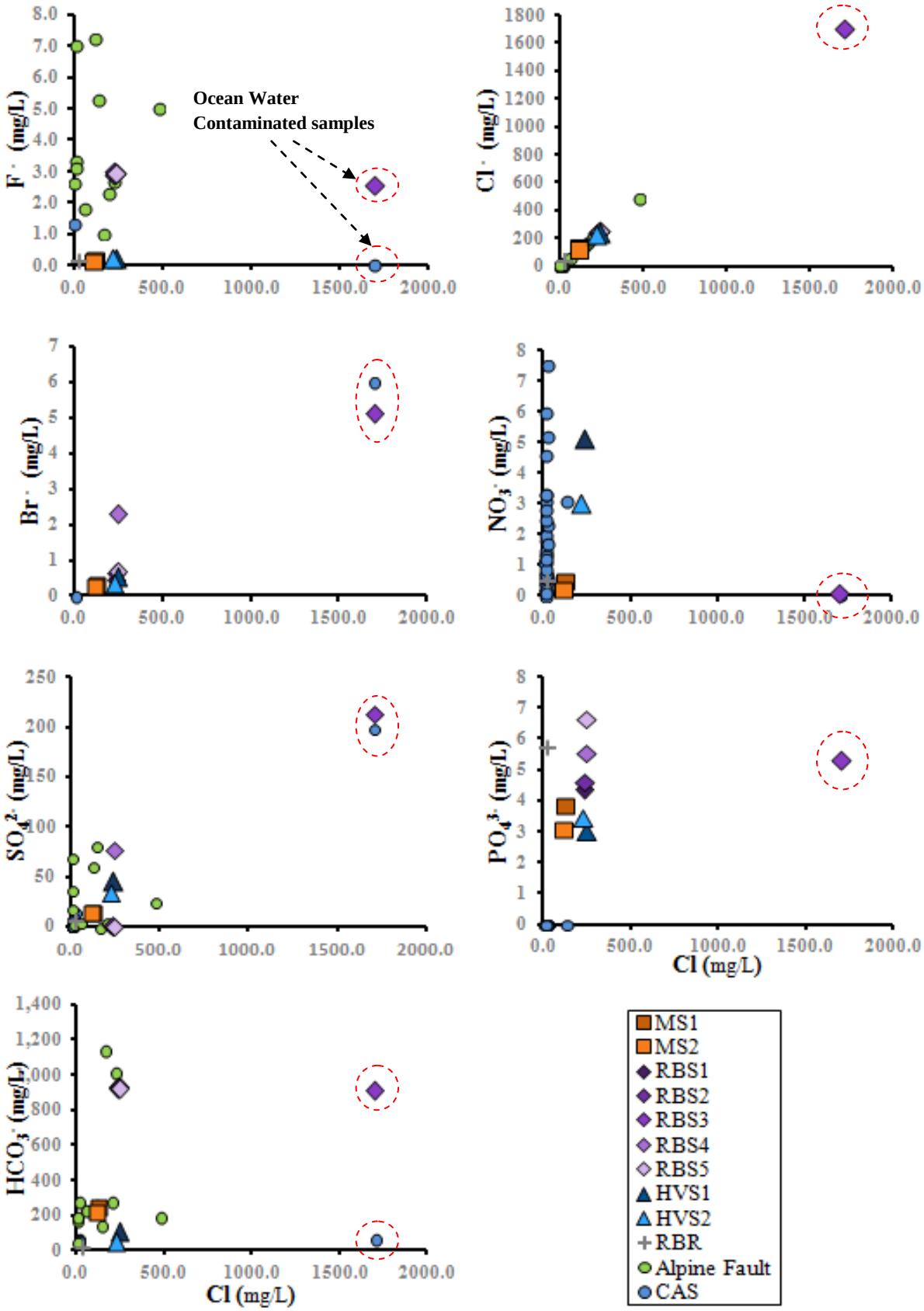

Figure 5.10: Anions versus Cl^- (mg/L) of Banks Peninsula warm springs. Samples are distinct from local rain (RBR) and groundwater (CAS) show similar trends to Alpine Fault thermal waters. RBS3 shows signs of ocean water contamination exhibiting similar trends to a known salt water contaminated well within the CAS. reported by Hayward (2002). Additional data from Barnes et al. (1978), Hayward (2002), Aitchison-Earl et al. (2003), Hanson and Abraham (2009), and Environment Canterbury (2014).

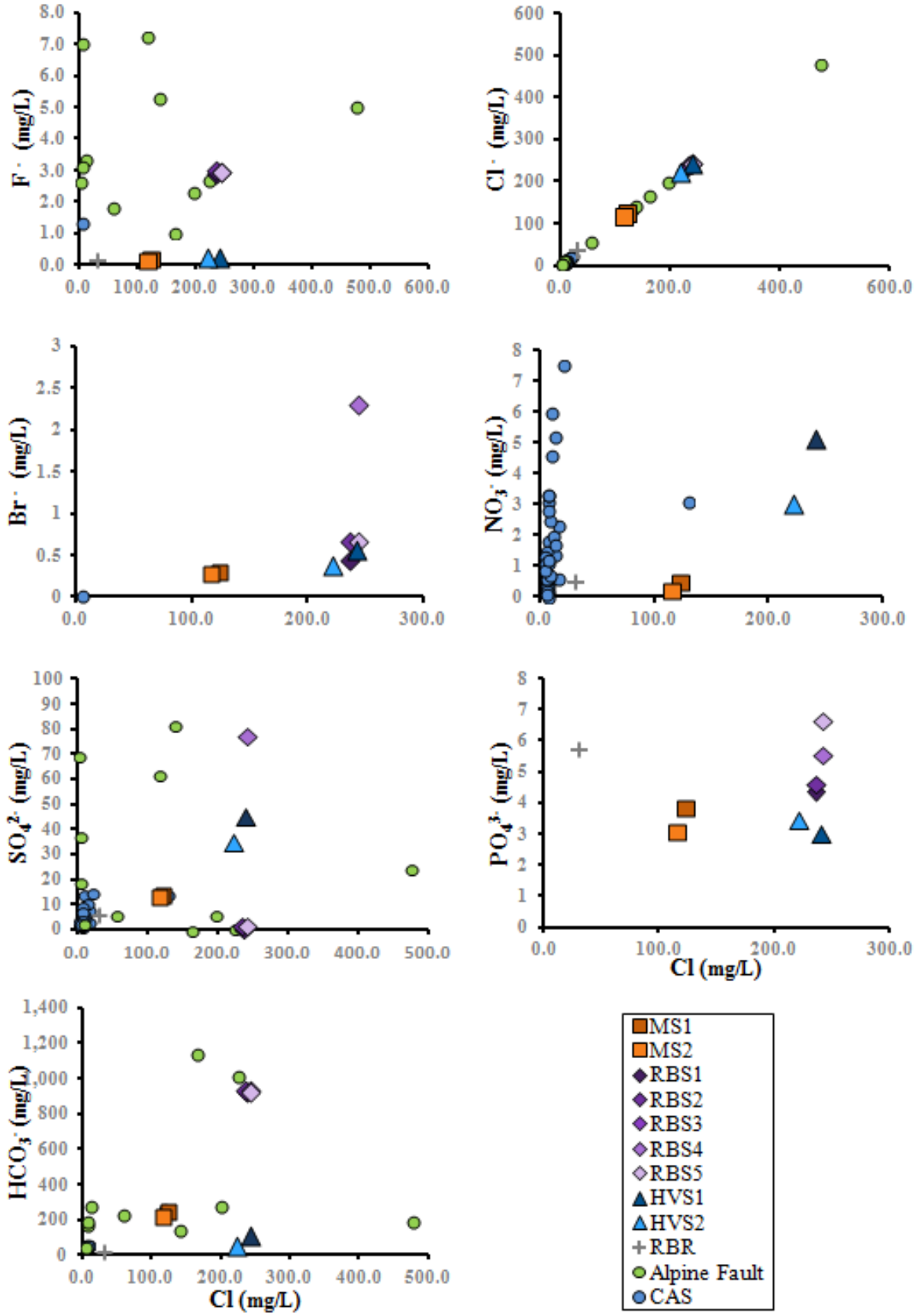

Figure 5.11: Banks Peninsula warm springs anion data versus Cl (mg/L) without ocean water contaminated samples. Both Motukarara and Hillsborough Valley samples exhibit similar trends with Rapaki Bay samples exhibiting higher concentrations. All of the Banks Peninsula samples plot within the range of the Alpine Fault springs and are chemically distinct from local groundwater (CAS) and rain (RBR)

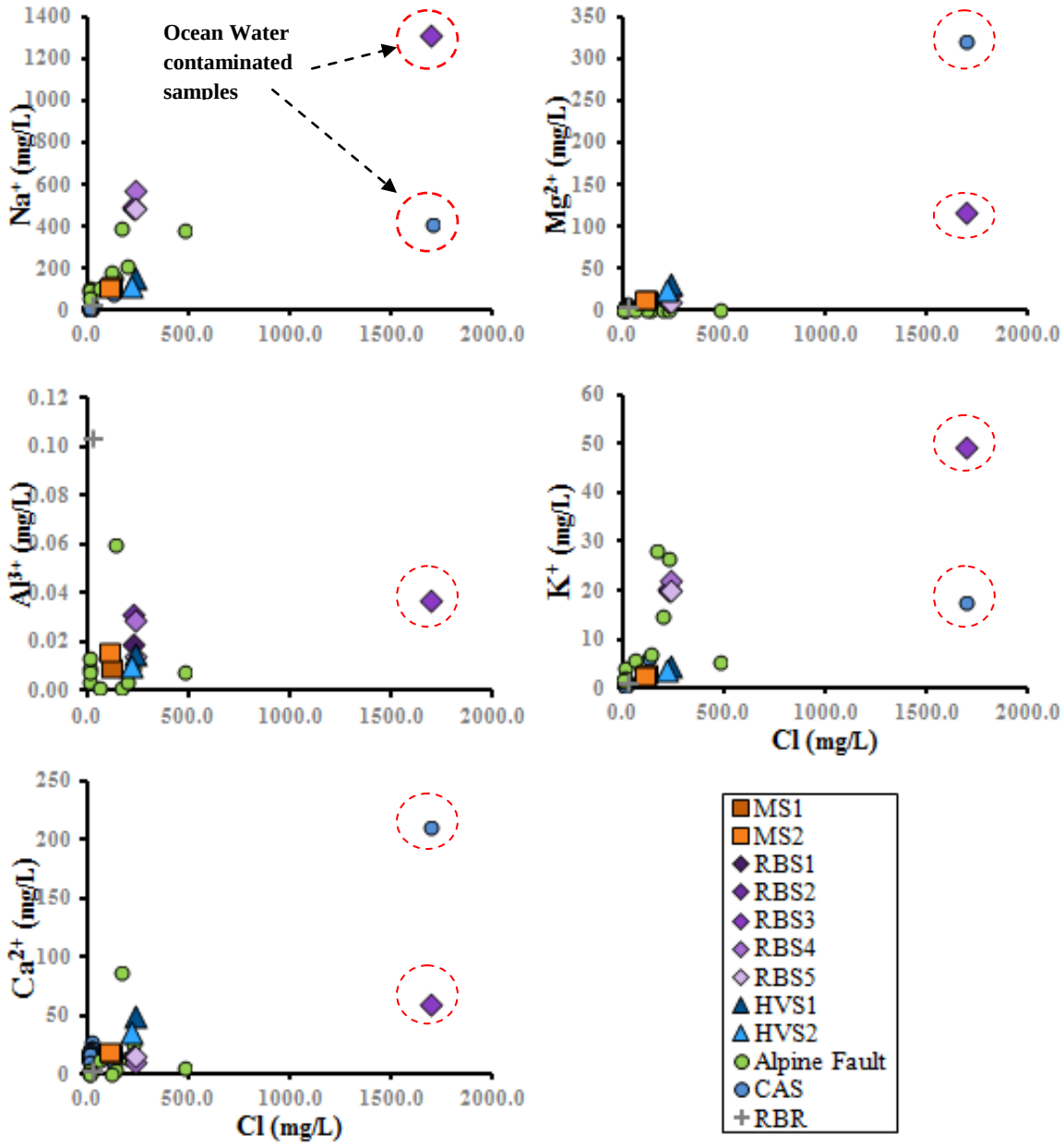

Figure 5.12: Cation versus Cl^- (mg/L) of Banks Peninsula warm springs. Additional data from Barnes et al. (1978), Hayward (2002), Aitchison-Earl et al. (2003), Hanson and Abraham (2009), and Environment Canterbury (2014). Ocean water contamination can be seen in the RBS3 sample which exhibits similar trends to the known salt water contaminated well of the CAS (outlined in red).

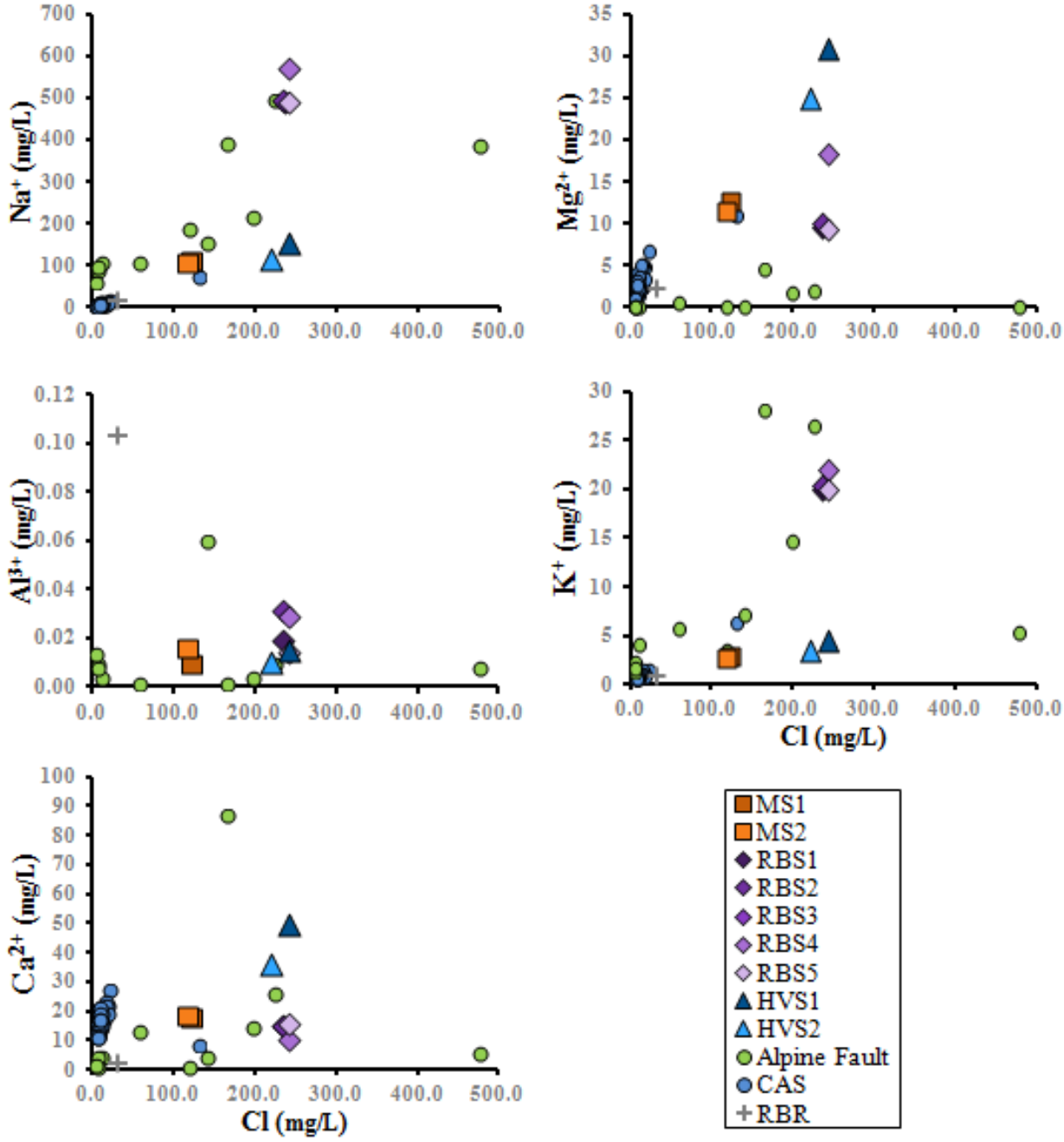

Figure 5.13: Banks Peninsula warm springs cation data versus Cl (mg/L) without ocean water contaminated samples. Banks Peninsula warm springs plot in a similar region to Alpine Fault thermal waters, and are distinct to local groundwater (CAS) and rain (RBR)

5.2.2 Water Isotopic Studies

The warm springs water plot along the Global Mean Water Line (GMWL) indicating meteoric origin (Figure 5.15). However, the position along the GMWL of the Banks Peninsula warms springs indicates a different source from the local groundwater and meteoric rain. The $\delta^{18}O$ and

δD values range from -8.3to -9.26, and -60.15 to -64.19 (‰ V-SMOW) respectively (Figure 5.16). This plots within the same region as the Alpine Fault thermal springs; such as Copland River, as well as thermal meteoric waters observed at *The Geysers*, California, indicating a similar origin that is distinct from local rain and Banks Peninsula groundwater. However some overlap is observed between the Hillsborough Valley samples and the lower range of the Waimakariri and Canterbury Aquifer System (CAS) samples, indicating potential evidence for groundwater mixing as is observed in Figure 5.14.

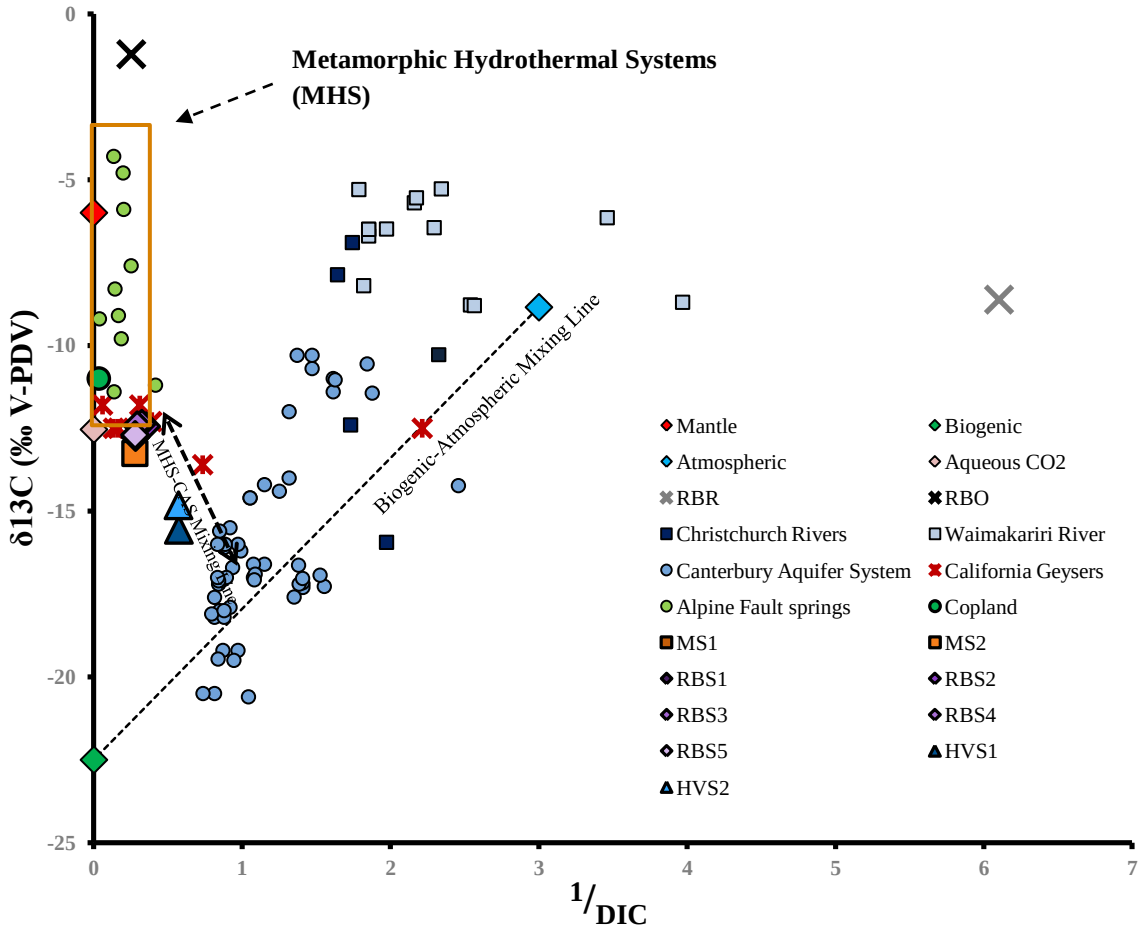

Figure 5.14: $\delta^{13}C$ (‰ V-PDV) versus $^{1}/_{DIC}$ gives an indication of heat source for the Banks Peninsula Warm Springs. The Rapaki springs plot within the region of Metamorphic Hydrothermal Systems (MHS); the same region as the Alpine Fault geothermal system, especially Copland River, and *The Geysers*, California, U.S.A.,) (Barnes et al., 1978; Donnelly-Nolan et al., 1993)**. The Motukarara and Hillsborough Valley samples show evidence of mixing between the MHS heat signature and the local Canterbury Aquifer System (CAS)** (Stewart, 2012)**. This mixing between the MHS and CAS is also evident within the $\delta^{18}O$ and δD signatures.**

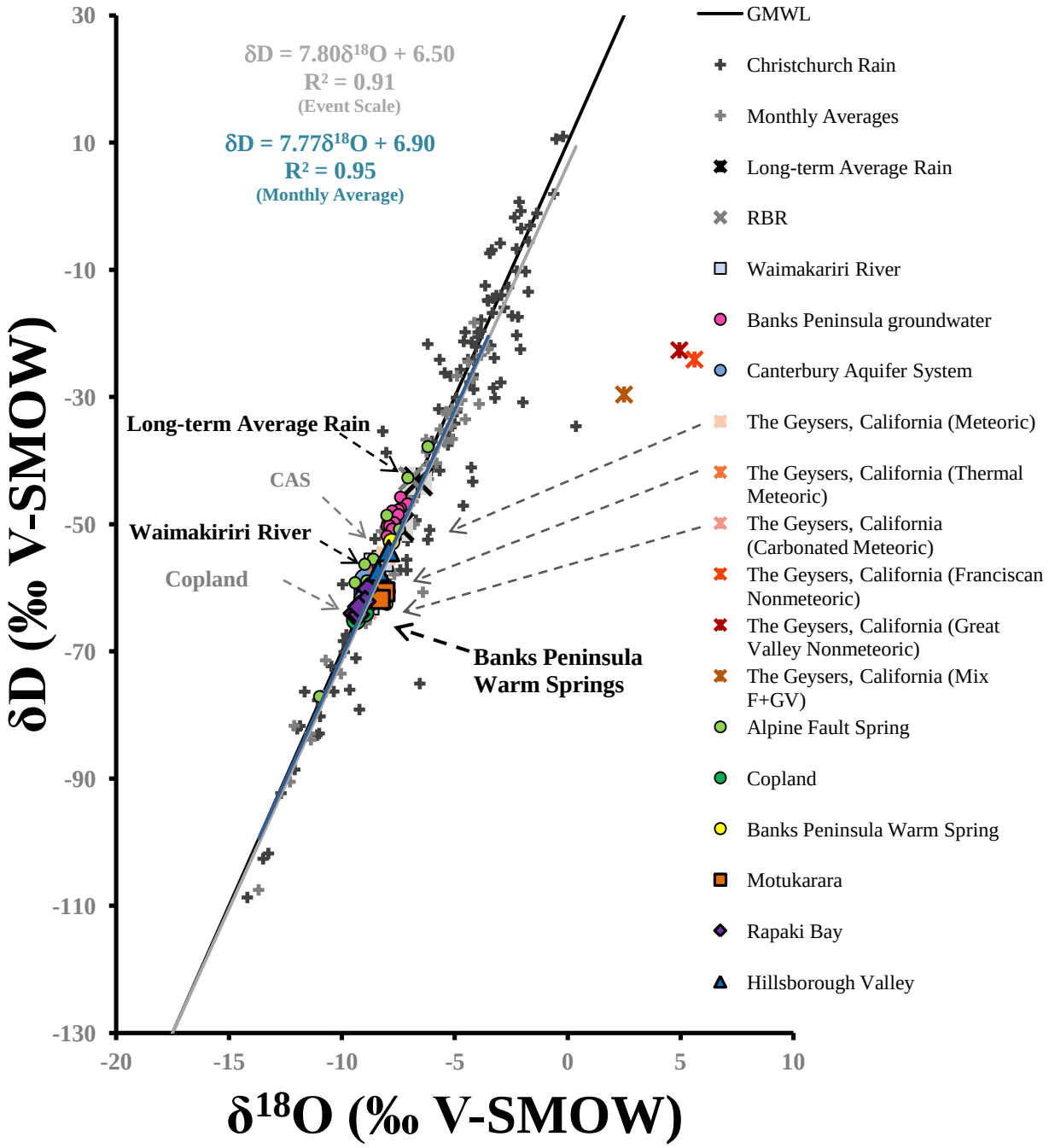

Figure 5.15: Isotopic bi-variant plot $\delta^{18}O$ versus δD. Banks Peninsula Warm Springs are seen to plot along the Global mean Water Line (GMWL) indicating a meteoric origin to the water. The warms springs exhibit similar signatures to the Copland thermal spring (Alpine Fault hydrothermal system) and thermal meteoric waters from *The Geysers*, California, U.S.A. The waters are isotopically distinct from local rain (RBR, monthly average, and event scale samples) and Banks Peninsula groundwater, yet have some overlap with the Canterbury Aquifer System (CAS), and Waimakariri River samples both of which are sourced from rain within Southern Alps (Barnes et al., 1978; Donnelly-Nolan et al., 1993; Reyes et al., 2010; Stewart, 2012; Scott, 2014). The observed spread between the three different sample sites, Motukarara, Rapaki Bay, and Hillsborough Valley, reflects the warm spring waters interaction with the local groundwater.

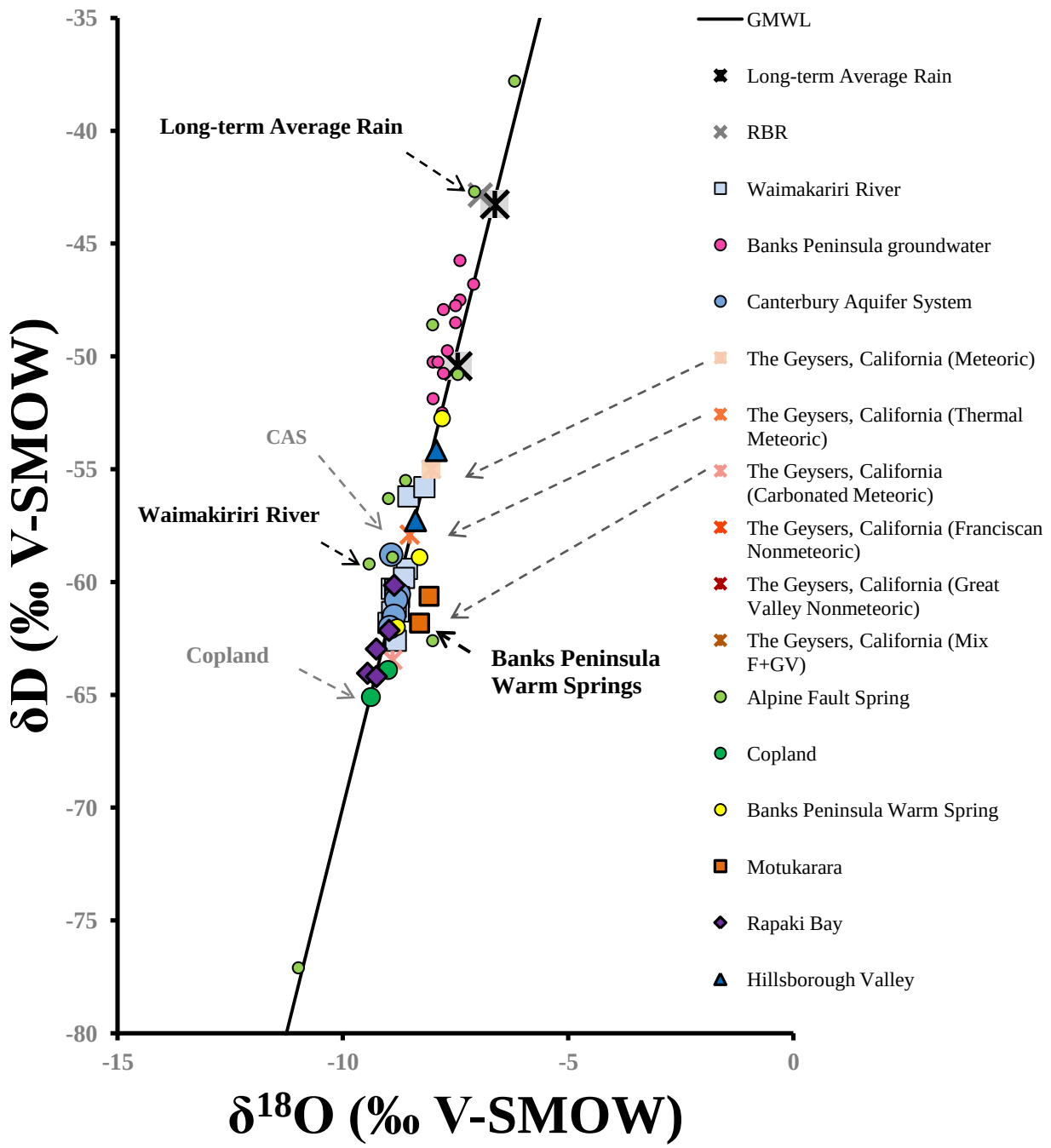

Figure 5.16: Close up of Banks Peninsula warm springs $\delta^{18}O$ versus δD values. Values for the warm springs are seen to overlap with those from the Canterbury Aquifer System (CAS) and Waimakariri River, yet plot within the same range of the Alpine Fault Springs, reflecting mixing with the CAS.

$\delta^{13}C_{(CO_2)}$ of the water samples varies for each sample location. Ranging from -6.03 at Rapaki Bay to -15.06 in Hillsborough Valley (Table 5.1, Figure 5.14), the warm springs form a linear mixing line between a Metamorphic Hydrothermal System (MHS) and Canterbury Aquifer

System (CAS) isotopic signature. The position of each of the warm springs localities to the presence of the CAS is evident in the amount of groundwater mixing in the water samples, with the two springs situated on the outer flanks of the Lyttelton Volcanic complex exhibiting the greatest amount of CAS mixing.

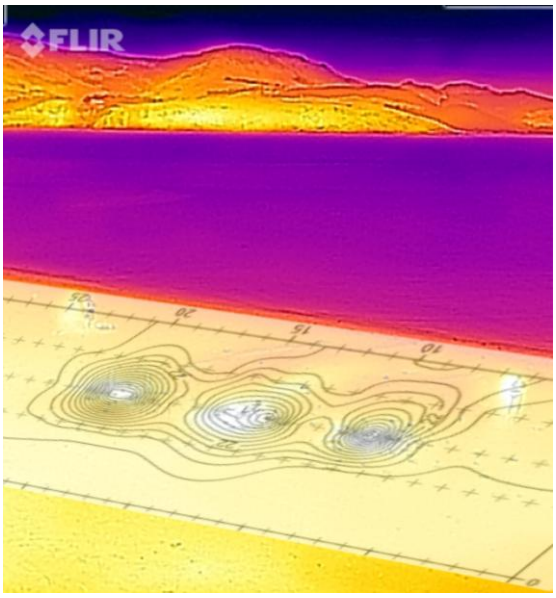

Figure 5.16: Temperature contour overlain on IR image of RBS2 (right), RBS3 (centre), and RBS4 (left). Contours from the temperature survey are seen to match the surface expression of the springs.

5.3 Temperature

A ground temperature survey was undertaken at the Rapaki Bay site. The survey area had an average temperature of 21.97 ± 3.44 °C, ranging from 16.4-34.8 °C at 10 cm depth (Table 5.1). Figures 5.17 and 5.18 reveal the distinct relationship between soil temperature and the location of the warm springs, with temperatures increasing around the springs as well as being elevated in the downflow direction of the water.

5.4 Gas

The initial gas survey was carried out around the three dominant central springs RBS2-RBS4 at the end of March 2015. A supplementary survey was undertaken late January 2016 to include RBS1 and RBS5 as well as other notable points from the temperature survey (Figure 5.18). The carbon dioxide (CO_2) flux averaged at 6.931 ± 10.189 $gm^{-2}day^{-1}$, $\delta^{13}C$ -19.81 ± 5.074 (Figure 5.19) with the highest flux being 39.694 ± 5.977 $gm^{-2}day^{-1}$. Majority of the survey area was considered low flux, with 31% of survey points having a flux > 0.1 $gm^{-2}day^{-1}$; and 70% of those measured with the

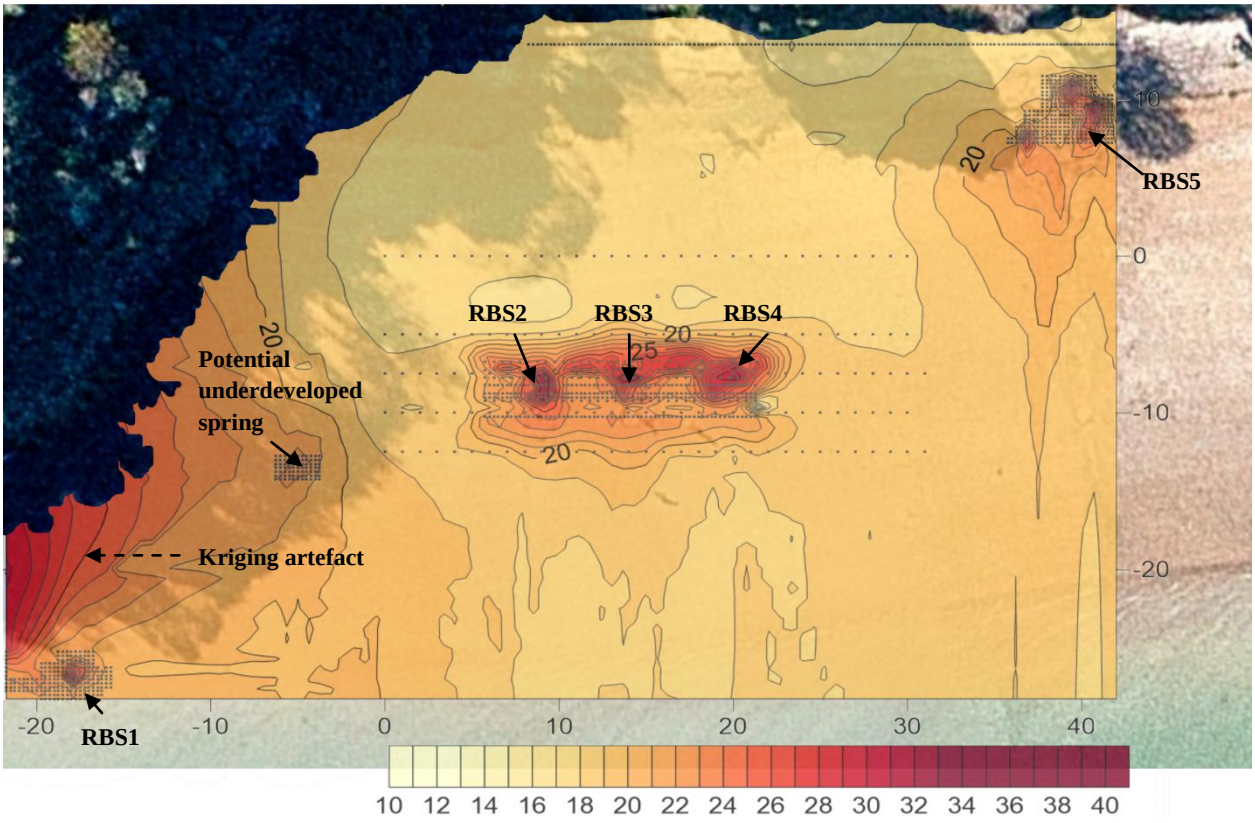

Figure 5.18: Rapaki Bay temperature Survey. Position of the warm springs correlates to increases in temperature. Bottom left RBS1, centre left RBS2, centre RBS3, centre right RBS4, top right RBS5. The increased temperature observed in the bottom left, above RBS1 is kriging artefact from processing. The increased temperature between RBS1 and RBS2 may reflect the development of a newer spring.

IRGA-CRDS being < 5 $gm^{-2}day^{-1}$. A strong correlation is seen between the areas of higher flux and the position of the warm springs (Figure 5.20A), which echoes what is observed in the temperature survey (Figure 5.18). Isotopically the $\delta^{13}C_{CO_2}$ sis not distinguished by any magmatic, biogenic or atmospheric signature. The values plot at the lower end of the metamorphic hydrothermal source band slightly below *The Geysers*, California samples, but within the non-biogenically mixed CO_2 range of Wanganui warm spring (Alpine Fault hydrothermal system; Figure 5.19; Bergfeld et al., 2001; Hanson et al., unpublished.a). The soil-gas flux data forms a linear band typical of a non-mixed source. Several of the more depleted isotopic samples, were the sites associated with methane (CH_4). In particular two samples from the soil-gas flux survey exhibit isotopic signatures that plot within the -30 ‰ (V-PDV) range. This lower isotopic value is

attributed to the incorporation of degratated CH_4 $\delta^{13}C$, which is naturally less stable and more isotopically depleted than $\delta^{13}C_{CO_2}$, within the effluxing CO_2 (Giggenbach et al., 1993).

Seven points sampled within the soil-gas flux survey were found to have detectable CH_4 (i.e. $CH_{4(g)} \geq 0.1$ $gm^{-2}day^{-1}$). These points were located either between RBS2 and RBS3 in the high CO_2 efflux area or around RBS1 (Figure 13B), the limited detection of CH_4 is reasonable with other studies, reflecting CH_4 as a less diffuse a gasthan CO_2 (Giggenbach et al., 1993; Bloomberg et al., 2014; Hanson et al., 2014b). The CH_4 flux readings recorded from both surveye averaged at 5.578 ± 12.101 $gm^{-2}day^{-1}$ with a $\delta^{13}C$ signature of -59.52 ± 1.48. Only the highest recorded efflux site was within the detection limits of the IRGA; averaging at 31.961 ± 1.32 $gm^{-2}day^{-1}$, $\delta^{13}C$ -59.97 ± 0.00 between IRGA and CRDS readings (Figure 5.20B). The CRDS CH_4 alarm was raised at one site around RBS5; unfortunately public utilisation and modification of the area surrounding the warm spring during the survey period resulted in abondonment of the site, resulting in no further samples being taken. Minor hydrogen sulphide ($H_2S_{(g)}$) was also detected around RBS1 however, the readings were at or below the detection limit of the equipment (0.02 ppm) and are therfore not reported here.

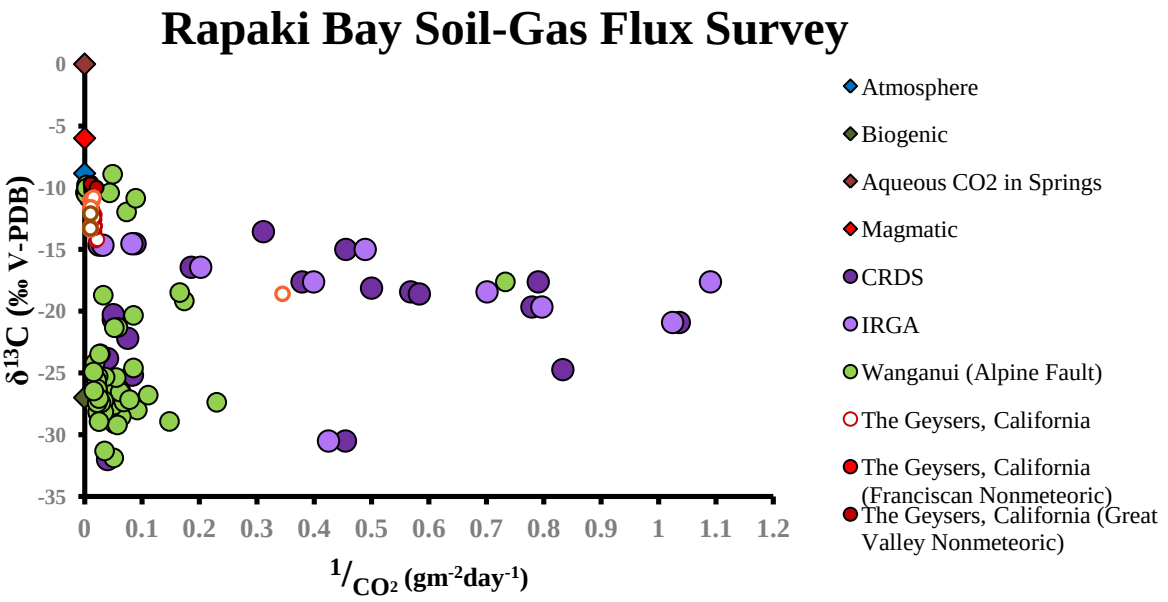

Figure 5.19: Isotopic trends of Rapaki Bay soil-gas flux survey compared to Wanganui (Alpine Fault thermal spring) and The Geysers, California (Lowenstern and Janik, 2003; Hanson et al., unpublished.a)

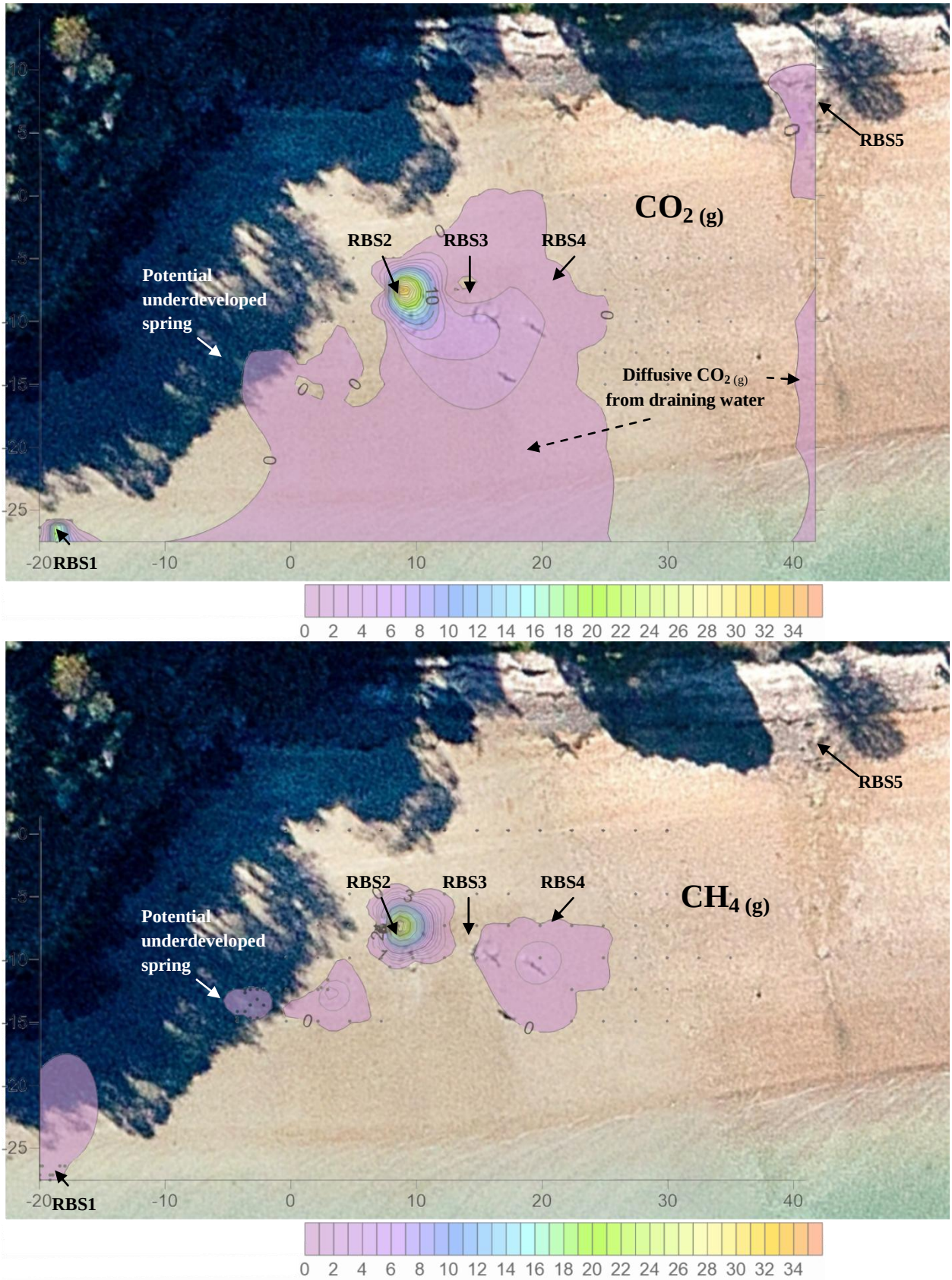

Figure 5.20: A) CO_2 soil-gas emissions from Rapaki Bay warm springs. High flux rates are associated with RBS1 and RBS2. B) CH_4 soil-gas emissions from Rapaki Bay warm springs. High flux rates are found between RBS2 and RBS3.

6. Discussion

6.1 Temporal Variation and Earthquake Inducement of the Banks Peninsula Warm Springs

The Canterbury Earthquake Sequence (CES), induced notable effects on the local groundwater within the Canterbury region, including the Banks Peninsula area (van Ballegooy et al., 2013). Post the CES, Canterbury experienced changes to its groundwater levels with many areas around the Peninsula experiencing elevated water levels. These changes in water and ground behaviour induced by the CES also affected the warm springs throughout the area; with locals reporting an increase of activity at the springs, citing increases of temperature, surface features, and gas emissions (Gorman, 2011; van Ballegooy et al., 2013). Reports also surfaced regarding the appearance of new springs within the Hillsborough Valley region. Situated on the outer flanks of the Peninsula, in close proximity to the inferred fault trace of the February 2011 Mw 6.2 earthquake (Figures 3.2 and 3.3), these new springs appeared throughout the valley along fissure traces generated from the resultant ground movement (Green, 2015). The effect of the CES to water and gas activity was seen as far inland as the Southern Alps; with Cox et al. (2015) reporting an increase in gaseous activity and temperature within the Copland thermal spring. The expansion and appearance of new springs, alongside local and Cox et al.'s (2015) observation of changing behaviour to the warm springs as a result of the CES event adds weight to Sewell et al.'s (1992) inference of a relationship between the placement of the warm springs within Banks Peninsula and the inherent faults present in the basement rock.

Despite the appearance of the new Hillsborough Valley springs as a result of the CES, most of the known warm springs within Banks Peninsula have been established for an extended period of time (Sewell et al., 1992a; Brown and Weeber, 1994). However, over time many of the warm springs have been redirected, diminished in terms of flow, or dried up

as a result of land development (Thain et al., 2006). Comparison of both the Motukarara and Rapaki Bay data (this thesis) against Brown and Weeber 's1994 and Reyes et al.'s 2010 studies, which encompass both warm springs prior to the CES event, reveals little temporal variation within the warm springs pre –post CES. This is in contrast to the increase in temperature and gaseous activity noted by the Banks Peninsula locals (Gorman, 2011) and the study by Cox et al. (2015); who inferred the observed change in activity at Copland, Alpine Fault geothermal system, to be a direct result of the CES. This disparity in data can be attributed to the four year gap between the sample collection of this study and CES event. Hence we can assume that the geochemical data presented in this thesis reflects the warm springs in their steady state (i.e. uninfluenced by the CES).

The only evidence retrieved from this study relating the warm springs back to the CES event is the classification of the new Hillsborough Valley springs as warm springs, and the near linear expansion of surficial features at the Motukarara and Rapaki Bay sites. The relationship between the Hillsborough Valley warm springs and their use of fault induced fissures as permeable conduits for fluid flow is apparent. If we infer this type of relationship to the generation and expansion of warm springs at both Motukarara and Rapaki Bay sites (Figure 6.1) in relation to the geochemistry of the warm springs we can start to understand the origin and fluid transportation of the Banks Peninsula geothermal system.

Observable increases in temperature and gas efflux from the warm springs in relation to the CES event, provides evidence towards increased permeability of the Banks Peninsula geothermal system. Sewell et al. (1992) when mapping the Peninsula inferred the semi-linear placement of the warm springs to reflect inherent faulting, aligned with the Canterbury horst system, within the underlying basement Rakaia Terrane, now recognised as the Gebbies Pass fault system (Ring and Hampton, 2012). Inherent faulting within the host rock is well known to act as conduits for geothermal fluid flow, while changes in stress within a fault has

been shown to affect the permeability of the system (Anderson, 2005; Tenthorey and Fitz Gerald, 2006). Taking into account the observed origin of the Hillsborough Valley springs, and the increases in temperature, gas efflux, and surface expression of both Motukarara and Rapaki Bay sites, as well as similar observed temperature and gas efflux changes within the Alpine Fault geothermal system; credence can be given to Sewell et al.'s (1992) interpretation for fault driven constraint on the Banks Peninsula hydrothermal system. However, the exact relationship between inherent faults and fractures present in the Rakia Terrane and Banks Peninsula Volcanic Complex with respect to permeability and fluid transportation is an area that requires further investigation.

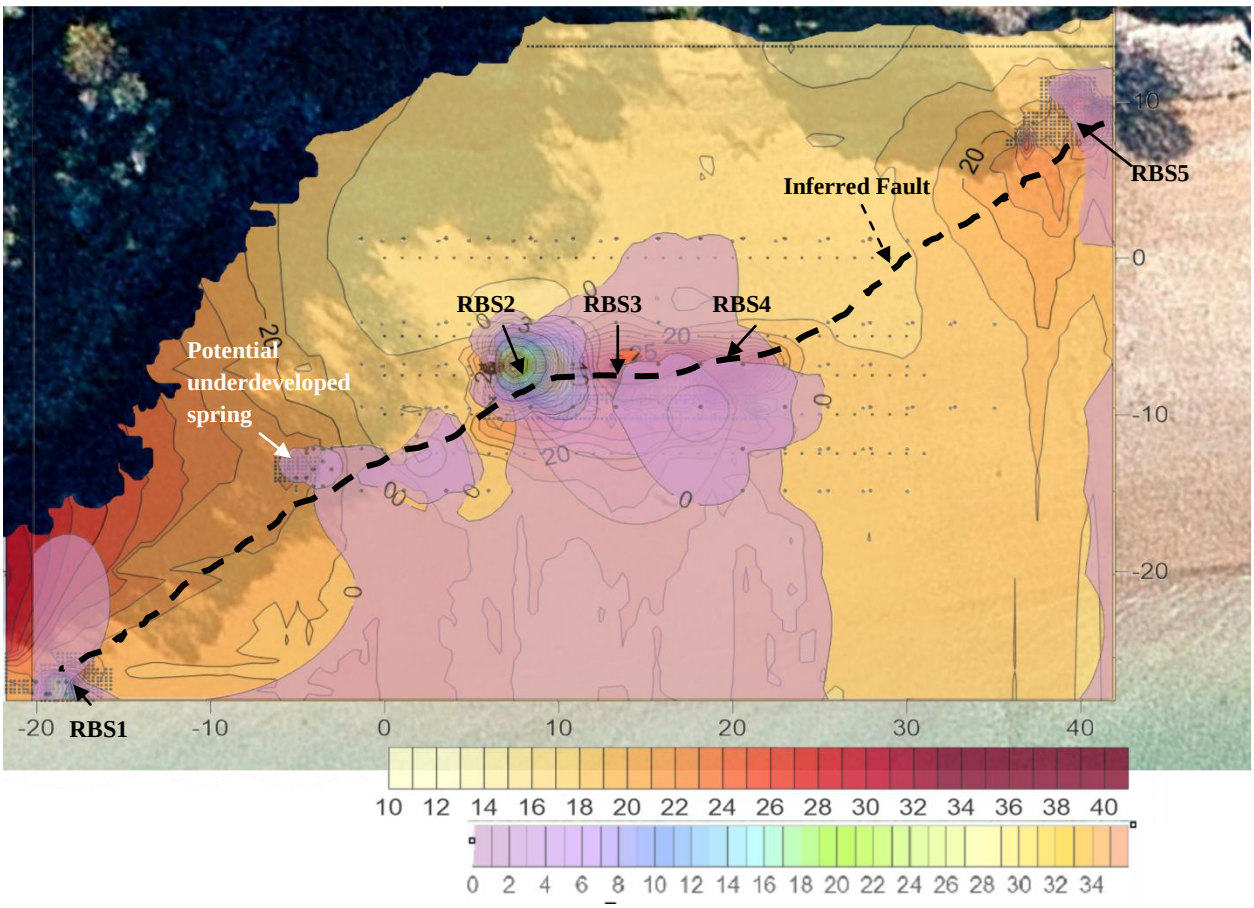

Figure 6.1: Results from the combined temperature and soil-gas flux surveys at Rapaki Bay with inferred fault trace.

6.2 Banks Peninsula, an Extension of the Alpine Fault Geothermal System

The Rakia Terrane is the largest basement terrane in New Zealand and underlies the Banks Peninsula Volcanics along with a significant portion of the South Island, including the Southern Alps (Mortimer, 2004). The Terrane comprised predominantly of quartzofeldspathic sandstone-mudstone is known for its structural complexity and is often described as being heavily fractured and faulted (Sewell et al., 1992a; Mortimer, 2004; Forsyth et al., 2008). It is within this structurally complex, heavily faulted terrane that both the Banks Peninsula and Alpine Fault geothermal systems operate.

There is a clear correlation between the Southern Alps geothermal springs and the warm springs located on Banks Peninsula in terms of their gas and water isotopic signatures and geochemistry. Both geothermal systems exhibit Na/HCO_3 type waters with high chloride concentrations. This is distinct from the Ca/HCO_3 type of local Canterbury groundwater and Alpine rainwater, and the Na/Cl type of the Banks Peninsula rainwater (Figure 5.5). The Hillsborough Valley samples plot within a different region to the other samples from this thesis (the Na/Cl region) but still reflect the water type of other Banks Peninsula springs previously sampled by Brown and Weeber (1994), that existed around the lower flanks of the Lyttelton volcanic complex. The lower HCO_3^{2-} concentrations of the sample resulting in a higher Na: Cl ratio reminiscent of the waters interaction with the low HCO_3, high Cl^- Birdlings Flat loess. Despite both the Hillsborough Valley and Rapaki rain water samples plotting in the same region, isotopically the two samples are distinct with the Hillsborough Valley samples exhibiting significantly more depleted $\delta^{18}O$, δD, and $\delta^{13}C$ signatures than RBR that are more in line with the other Banks Peninsula warm spring and Alpine Fault spring samples (Table 5.1, Figures 5.14 and 5.16).

The springs along the Southern Alps have been well studied and the source and mechanism well defined (Cox et al., 1997; Wannamaker, 2002; Campbell et al., 2004; Cox et

al., 2015). Isotopically and geochemically, the Banks Peninsula geothermal system plots within the same geochemical regions, which alludes to a similar source and mechanism.

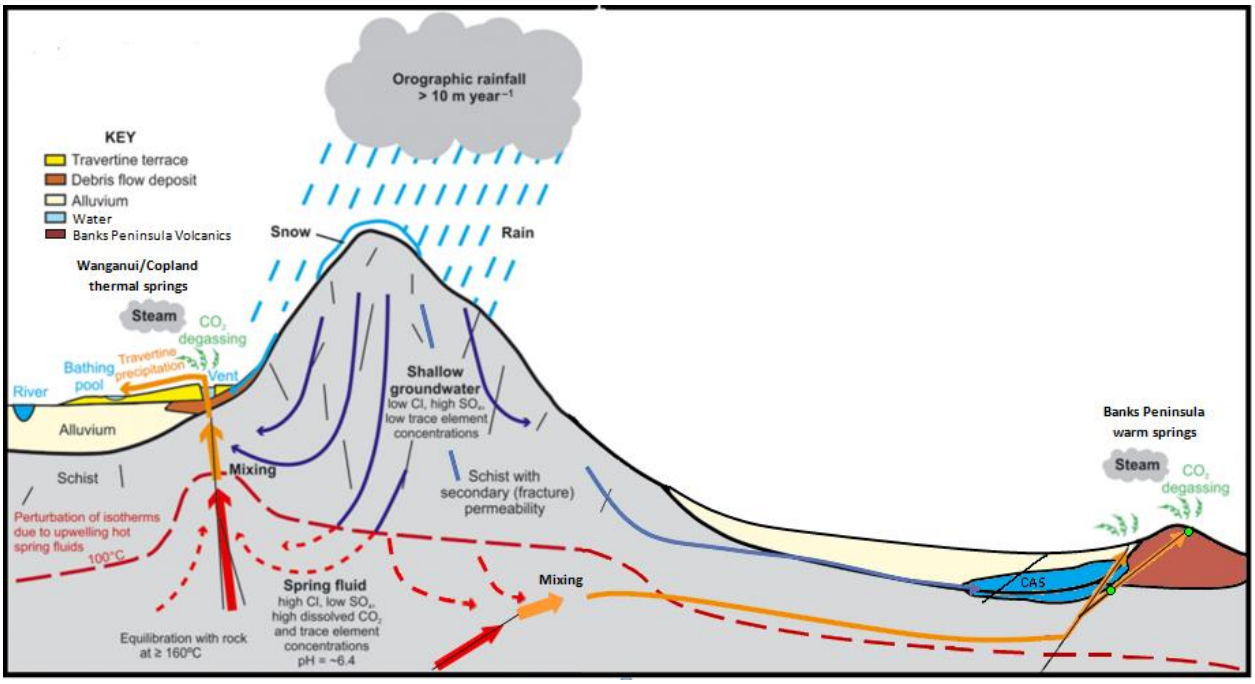

Figure 6.7: Cartoon of the proposed mechanism for Banks Peninsula warm springs. Image modified from (Cox et al., 2015).

Comparison of both systems against *The Geysers*, system in California, U.S.A. (Donnelly-Nolan et al., 1993; Bergfeld et al., 2001), one of the most well studied and understood metamorphic hydrothermal systems in the world reveals that what is geochemically observed at Banks Peninsula is indicative of metamorphic hydrothermal system, that is more likely an eastward extension of the Alpine Fault geothermal system feeding from the same metamorphic hydrothermal source rather than its own separate geothermal system (Figure 6.2).

The main disparity between the Alpine Fault geothermal system and the warm springs at Banks Peninsula is their difference in temperature, which can be rationalised when the distance of the flow path of the water from the heat source is considered. The travel path of the water within the Alpine Fault geothermal system is considered to be 6 km from the heat source to the surface (Campbell et al., 2004), a distance that is far less than between the Southern Alps and Banks Peninsula. Increasing the flow path between the heat source and

the spring; results in a greater loss of thermal energy, along with increased interaction with the surrounding bedrock and local groundwater; which consequently will result in the decreased temperature of the spring.

An extensive aquifer system (i.e. CAS) lies between the Southern Alps and Banks Peninsula extending into the same bedrock that provides a pathway for the geothermal fluid observed on the Peninsula. Consisting of shallow and deep aquifers and aquitards, the CAS predominantly interacts with varying forms of reworked torlesse in the form of the Canterbury gravels as well as the lower greywacke bedrock (Browne and Naish, 2003; Forsyth et al., 2008; Lough and Williams, 2009). Any water travelling through the Canterbury region towards Banks Peninsula from the Southern Alps is likely to be influenced by the CAS. Thus, the amount of mixing between the CAS/groundwater table and the transported geothermal fluid needs to also be taken into consideration when assessing the Banks Peninsula warm springs as part of the Alpine Fault geothermal system. Figure 5.13 depicts the amount of mixing between the metamorphic hydrothermal heat source and the CAS of the different Banks Peninsula warm springs. Notably, the Hillsborough Valley samples show a much greater mixing signature than the Motukarara and Rapaki Bay, reflecting their geographical relationship to the Christchurch-West Melton aquifer and the warm springs' increased susceptibility to groundwater influence from the surrounding loess. The Rapaki Bay samples, which exhibit the least amount of groundwater mixing plot within the same heat source region (metamorphic hydrothermal system) as that of the Alpine fault geothermal system, indicating a similar-identical heat source, plausible for springs belonging to the same system.

Reyes et al. (2010) interpreted the Banks Peninsula hydrothermal waters to reflect mixing of ocean water with the hydrothermal water. The warm spring waters' Na:Cl ratios in conjunction with their coastal setting supports this conclusion. However, when the data is

plotted as a function of mixing between freshwater and ocean water (Figures 5.7 and 6.3) a similar trend can be observed with the Alpine Fault spring water, a hydrothermal system known to have no ocean water infiltration. This, in conjunction with the Banks Peninsula samples isotopic signatures does not support ocean water mixing with the Banks Peninsula warm springs source water; the notable exception being surface mixing of spring and ocean water at Rapaki Bay.

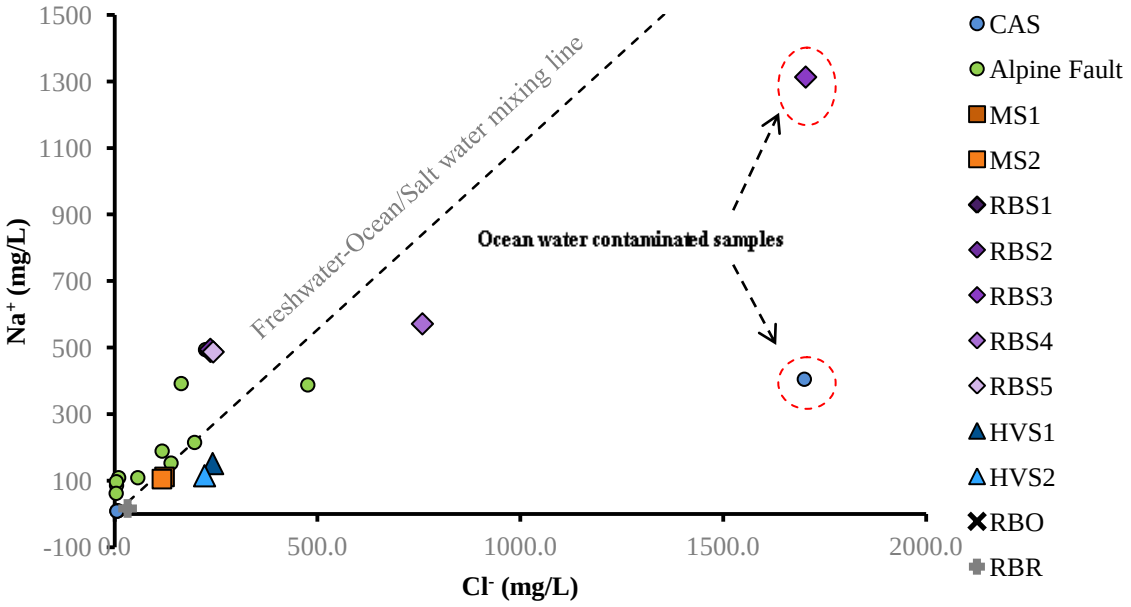

Figure 6.3: Close up of Figure 5.7; warm spring samples exhibit similar trends and plot within a similar region to the Alpine Fault springs, water known to not be contaminated by salt water.

The results seen in Figure 6.3, questions the generalised assumption of ~Na:Cl ratio representing salt water content within a sample. High concentrations of Na and Cl are typical for geothermal waters (Navarro et al., 2011; Gibson and Hinman, 2013). For salt water to be present within the Alpine Fault hydrothermal system the supposed "salt water" would have to be sourced from rock-water interactions with the greywacke host rock. Comparison of the TDS between the CAS and Alpine Fault springs (Figure 5.8), two systems hosted by the same greywacke lithology and meteoric water source, supports greater water-rock interaction in the

hydrothermal samples, which is intuitive considering the temperature differential between the samples. The TDS observed for the hydrothermal waters however, is relatively low for geothermal fluids, which would infer a low residence times with the greywacke host and therefore low water-rock interaction. This makes the source for the Na and Cl brine more likely to be associated with the source metamorphic hydrothermal waters that mix and heat the source meteoric water at depth. As the brine represents a fraction of the water sampled at the surface, questions need to be asked about the percentage of metamorphic hydrothermal fluid expressed in the surface waters, the water –rock interaction associated with the metamorphic hydrothermal fluid, and the extent of the fault network that enables the fluid to flow through the upper crust. This will provide a better understanding of "salt water" presence and interaction in hydrothermal systems.

7. Conclusions

The warm springs present in Bank Peninsula are fed from a metamorphic hydrothermal system that is mixed with high altitude meteoric water. This type of geothermal mechanism is observed throughout the South Island, with majority of the thermal springs relating back to the Alpine Fault geothermal system. What is geochemically observed at Banks Peninsula is a representation of an eastward extension of the Alpine Fault geothermal system (Figure 6.2). The lower temperatures and slight isotopic and geochemical variation of the Banks Peninsula warm springs compared to other regions of the Alpine Fault system; reflects the increased distance of travel, as well as greater interaction with the local groundwater table (i.e. the CAS). Perturbation from the CES to the pre-established warm springs alongside the formation of the Hillsborough Valley warm springs, provided insight into the structural controls behind the warm springs lending credibility to Sewell et al.'s (1992) inference of inherent faults beneath the Peninsula being exploited as permeable conduits for fluid transport and flow of the system.

Table 7.2: Research Questions and Answers

Questions	Answers
What is the CO_2 and CH_4 flux for the warm springs? What is influencing the elevated temperatures of the warm springs?	• $\delta^{13}C$ from both CO_2 and CH_4 analysis points towards a metamorphic hydrothermal heat source. Comparison to *The Geysers*, geothermal field, California and Wanganui, Southern Alps geothermal system reflects the Banks Peninsula gas flux to be of similar origin.
What is the source of the Banks Peninsula spring water?	• The bivariate $\delta^{18}O$ vs. δD plot reveals that the water is meteoric in origin, with a similar signature to that of the Alpine Fault geothermal system. • From the $\delta^{13}C$ water values, the warm springs reflect mixing between a metamorphic hydrothermal source and the Canterbury aquifer system (CAS). • Geochemically the warm springs exhibit similar chemical traits to the Alpine Fault system with deviations in the samples reflecting the amount of CAS influence on the sample.

8 REFERENCES

Aitchison-Earl, P., Ettema, M., Hanson, C., Hayward, S., Larking, R., Sanders, R., Scott, D., and Veltman, A., 2003, Report No. R04/18: Coastal aquifer saltwater intrusion assessment guidelines:.

Altaye, E., 1989, The Geology and Geochemistry of the North-Eastern Sector of Lyttleton Volcano, Banks Peninsula, New Zealand: University of Canterbury, 1-157 p.

Anderson, M.P., 2005, Heat as a ground water tracer: Ground Water, v. 43, no. 6, p. 951–968, doi: 10.1111/j.1745-6584.2005.00052.x.

van Ballegooy, S., Cox, S.C., Agnihotri, R., Reynolds, T., Thurlow, C., Rutter, H.K., Scott, D.M., Begg, J.G., and McCahon, I., 2013, Median Water Table Elevation in Christchurch and Surrounding Area after the 4 September 2010 Darfield Earthquake:.

Bannister, S., Fry, B., Reyners, M., Ristau, J., and Zhang, H., 2011, Fine-scale Relocation of Aftershocks of the 22 February Mw 6.2 Christchurch Earthquake using Double-difference Tomography: Seismological Research Letters, v. 82, no. 6, p. 839–845, doi: 10.1785/gssrl.82.6.839.

Barnes, I., Downes, C.J., and Hulston, J.R., 1978, Warm springs, South Island, New Zealand, and their potentials to yield laumontite: American Journal of Science, v. 278, no. 10, p. 1412–1427, doi: 10.2475/ajs.278.10.1412.

Beavan, J., Fielding, E., Motagh, M., Samsonov, S., and Donnelly, N., 2011, Fault Location and Slip Distribution of the 22 February 2011 Mw 6.2 Christchurch, New Zealand, Earthquake from Geodetic Data: Seismological Research Letters, v. 82, no. 6, p. 789–799, doi: 10.1785/gssrl.82.6.789.

Bergfeld, D., Goff, F., and Janik, C.J., 2001, Carbon isotope systematics and CO2 sources in The Geysers-Clear Lake region, northern California, USA: Geothermics, v. 30, no. 2-3, p. 303–331, doi: 10.1016/S0375-6505(00)00051-1.

Bierlein, F.P., and Craw, D., 2009, Petrogenetic character and provenance of metabasalts in the aspiring and Torlesse Terranes, South Island, New Zealand: Implications for the gold endowment of the Otago Schist? Chemical Geology, v. 260, no. 3-4, p. 330–344, doi: 10.1016/j.chemgeo.2009.01.016.

Bloomberg, S., Werner, C., Rissmann, C., Mazot, A., Horton, T., Graveley, D., Kennedy, B., and Oze, C., 2014, Soil CO2 emissions as a proxy for heat and mass flow assessment, Taupo Volcanic Zone, New Zealand: Geochemistry, Geophysics, Geosystems: G3, v. 15, no. 12, p. 4885–4904, doi: 10.1002/2014GC005327.Received.

Brown, L.J., and Weeber, J.H., 1994, Hydrogeological implications of geology at the boundary of Banks Peninsula volcanic rock aquifers and Canterbury Plains fluvial gravel aquifers: New Zealand Journal of Geology and Geophysics, v. 37, no. March 2015, p. 181–193, doi: 10.1080/00288306.1994.9514613.

Browne, G.H., and Naish, T.R., 2003, Facies development and sequence architecture of a late Quaternary fluvial-marine transition, Canterbury Plains and shelf, New Zealand: Implications for forced regressive deposits: Sedimentary Geology, v. 158, no. 1-2, p. 57–86, doi: 10.1016/S0037-0738(02)00258-0.

Campbell, J.R., Craw, D., Frew, R., Horton, T., and Chamberlain, C.P., 2004, Geochemical signature of orogenic hydrothermal activity in an active tectonic intersection zone, Alpine Fault, New Zealand: Mineralium Deposita, v. 39, p. 437–451, doi: 10.1007/s00126-004-0421-4.

Chiodini, G., Cioni, R., Guidi, M., Raco, B., and Marini, L., 1998, Soil CO2 flux measurements in volcanic and geothermal areas: Applied Geochemistry, v. 13, no. 5, p. 543–552, doi: 10.1016/S0883-2927(97)00076-0.

Christchurch City Council, 2009, Christchurch City Council WATER SUPPLY STRATEGY

2009 - 2039 28:.
Cox, S.C., Craw, D., and Chamberlain, C.P., 1997, Structure and fluid migration in a late Cenozoic duplex system forming the Main Divide in the central Southern Alps, New Zealand: New Zealand Journal of Geology and Geophysics, v. 40, no. 3, p. 359–373, doi: 10.1080/00288306.1997.9514767.
Cox, S.C., Menzies, C.D., Sutherland, R., Denys, P.H., Chamberlain, C., and Teagle, D. a. H., 2015, Changes in hot spring temperature and hydrogeology of the Alpine Fault hanging wall, New Zealand, induced by distal South Island earthquakes: Geofluids, v. 15, no. 1-2, p. 216–239, doi: 10.1111/gfl.12093.
Donnelly-Nolan, J.M., Burns, M.G., Goff, F.E., Peters, E.K., and Thompson, J.M., 1993, The Geysers-Clear Lake area, California: thermal waters, mineralization, volcanism, and geothermal potential: Economic Geology, v. 88, no. 2, p. 301–316, doi: 10.2113/gsecongeo.88.2.301.
Dorsey, C.J., 1988, the Geology and Geochemistry of Akaroa Volcano, Banks Peninsula, New Zealand: University of Canterbury, 278 p.
Environment Canterbury, 2011, Natural hazards:.
Environment Canterbury, G.Q.T., 2014, Report No. R14/68: Christchurch Groundwater Quality Monitoring 2013:.
Forsyth, P.J., Barrell, D.J.A., and Jongens, R., 2008, Geology of the Christchurch Area: Institute of Geological & Nuclear Sciences Ltd., Lower Hutt, New Zealand.
Gibson, M.L., and Hinman, N.W., 2013, Mixing of hydrothermal water and groundwater near hot springs, Yellowstone National Park (USA): hydrology and geochemistry: Hydrogeology Journal, v. 21, no. 4, p. 1–15, doi: 10.1007/s10040-013-0965-4.
Giggenbach, W.F., 1988, Geothermal solute equilibria. Derivation of Na-K-Mg-Ca geoindicators: Geochimica et Cosmochimica Acta, v. 52, p. 2749–2765, doi: 10.1016/0016-7037(88)90143-3.
Giggenbach, W.F., 1992, Isotopic shifts in waters from geothermal and volcanic systems along convergent plate boundaries and their origin: Earth and Planetary Science Letters, v. 113, p. 495–510, doi: 10.1016/0012-821X(92)90127-H.
Giggenbach, W.., Sano, Y., and Wakita, H., 1993, Isotopic composition of helium, and CO2 and CH4 contents in gases produced along the New Zealand part of a convergent plate boundary: Geochimica et Cosmochimica Acta, v. 57, no. 14, p. 3427–3455, doi: 10.1016/0016-7037(93)90549-C.
Gorman, P., 2011, Surging springs not a sign of volcanic activity: The Press, p. 4–5.
Green, M., 2015, Hydrogeological investigation of earthquake related springs in the Hillsborough valley, Christchurch, New Zealand: University of Canterbury, 125 p.
Griffiths, E., 1973, Loess of Banks Peninsula: New Zealand Journal of Geology and Geophysics, v. 16, no. 3, p. 657–675, doi: 10.1080/00288306.1973.10431388.
Hampton, S.J., 2010, Growth, Structure and Evolution of the Lyttleton Volcanic Complex, Banks Peninsula, New Zealand: University of Canterbury, 1-330 p.
Hampton, S.J., and Cole, J.W., 2009, Lyttelton Volcano, Banks Peninsula, New Zealand: Primary volcanic landforms and eruptive centre identification: Geomorphology, v. 104, no. 3-4, p. 284–298, doi: 10.1016/j.geomorph.2008.09.005.
Hanson, C., and Abraham, P., 2009, Report No. R09/39: Depth and spatial variation in groundwater chemistry - Central Canterbury Plains:.
Hanson, M.C., Horton, T.W., and Oze, C., unpublished.a, Soil CO2 flux and isotopic surveys to identify and characterize low enthalpy springs associated with the Alpine Fault, New Zealand:.
Hanson, M.C., Oze, C., and Horton, T.W., unpublished.b, Cavity Ring Down Spectroscopy for the Rapid Estimation of □ 13 C of Soil CO 2 Flux in H 2 S-rich Geothermal Areas:.

Hanson, M.C., Oze, C., and Horton, T.W., 2014a, Identifying blind geothermal systems with CO2 surveys: Applied Geochemistry, v. awaiting p, doi: http://dx.doi.org/10.1016/j.apgoechem.2014.08.009.

Hanson, M.C., Oze, C., and Horton, T.W., 2014b, Identifying blind geothermal systems with soil CO2 surveys: Applied Geochemistry, v. 50, p. 106–114, doi: 10.1016/j.apgeochem.2014.08.009.

Hayward, S. a, 2002, Report No. U02/47 part I: Christchurch-West Melton Groundwater Quality : A review of groundwater quality monitoring data from January 1986 to March 2002:.

Hoernle, K., White, J.D.L., van den Bogaard, P., Hauff, F., Coombs, D.S., Werner, R., Timm, C., Garbe-Schönberg, D., Reay, a., and Cooper, a. F., 2006, Cenozoic intraplate volcanism on New Zealand: Upwelling induced by lithospheric removal: Earth and Planetary Science Letters, v. 248, p. 335–352, doi: 10.1016/j.epsl.2006.06.001.

Hoke, L., Poreda, R., Reay, a., and Weaver, S.D., 2000, The subcontinental mantle beneath southern New Zealand, characterised by helium isotopes in intraplate basalts and gas-rich springs: Geochimica et Cosmochimica Acta, v. 64, no. 14, p. 2489–2507, doi: 10.1016/S0016-7037(00)00346-X.

Kaiser, A., Holden, C., Beavan, J., Beetham, D., Benites, R., Celentano, A., Collett, D., Cousins, J., Cubrinovski, M., Dellow, G., Denys, P., Fielding, E., Fry, B., Gerstenberger, M., et al., 2012, 6.2 Christchurch earthquake of February 2011: preliminary report: New Zealand Journal of Geology and Geophysics, v. 55, no. 1, p. 67–90, doi: 10.1080/00288306.2011.641182.

Lough, H., and Williams, H., 2009, Report No. R09/45: Vertical flow in Canterbury groundwater systems and its significance for groundwater management:.

Lowenstern, J.B., and Janik, C.J., 2003, The origins of reservoir liquids and vapors from The Geysers geothermal field, California (USA): Volcanic, Geothermal and Ore-forming …, p. 1–52.

Montelli, R., Nolet, G., Dahlen, A.F., and Masters, G., 2006, A catalogue of deep mantle plumes: New results from finite- frequency tomography: Geochemistry, Geophysics, Geosystems: G3, v. 7, no. 11, p. 1–69, doi: 10.1029/2006GC001248.

Mortimer, N., 2004, New Zealand's Geological Foundations: Gondwana Research, v. 7, no. 1, p. 261–272, doi: 10.1016/S1342-937X(05)70324-5.

Navarro, A., Font, X., and Viladevall, M., 2011, Geochemistry and groundwater contamination in the La Selva geothermal system (Girona, Northeast Spain): Geothermics, v. 40, no. 4, p. 275–285, doi: 10.1016/j.geothermics.2011.07.005.

Oxford Dictionary Oxford Press.

Reyes, A.G., 2010, Assessing the Flow of Thermal Waters in Low-Temperature Mineral Spring Systems in the South Island , New Zealand, *in* World Geothermal Congress, World Geothermal Congress, Bali, Indonessia, p. 25–29.

Reyes, A.G., and Britten, K., 2007, Variations in Chemical and Isotopic Compositions of Mineral Spring Systems in South Island , New Zealand: , no. 2001, p. 1–6.

Reyes, A.G., Christenson, B.W., and Faure, K., 2010, Sources of solutes and heat in low-enthalpy mineral waters and their relation to tectonic setting, New Zealand: Journal of Volcanology and Geothermal Research, v. 192, no. 3-4, p. 117–141, doi: 10.1016/j.jvolgeores.2010.02.015.

Reyes, A.G., and Jongens, R., 2005, Tectonic Settings of Low Enthalpy Geothermal Systems in New Zealand : An Overview, *in* World Geothermal Congress, p. 24–29.

Ring, U., and Hampton, S., 2012, Faulting in Banks Peninsula : tectonic setting and structural controls for late Miocene intraplate volcanism , New Zealand: Journal of the Geological Society, London, v. 169, p. 773–785, doi: 10.1144/jgs2011-167.Faulting.

Sanders, R. a, 1986, Hydrogeological studies of springs in Akaroa County, Banks Peninsula: University of Canterbury, 207 leaves (some folded) p.
Scott, L., 2014, Report No. R14/128: Review of Environment Canterbury ' s groundwater oxygen-18 data:.
Sewell, R.J., Hobden, B.J., and Weaver, S.D., 1993, Mafic and ultramafic mantle and deep crustal xenoliths from Banks Peninsula, South Island, New Zealand: New Zealand Journal of Geology and Geophysics, v. 36, no. 2, p. 223–231, doi: 10.1080/00288306.1993.9514570.
Sewell, R.J., Weaver, S.D., and Reay, M.B., 1992a, Geology of Banks Peninsula.: Institute of Geological & Nuclear Sciences Ltd, Lower Hutt, New Zealand.
Sewell, R.J., Weaver, S.D., and Reay, M.B., 1992b, Geology of Banks Peninsula. Scale 1:100 000. Institute of Geological Sciences geological map 3 (M. B. Reay, Ed.): Institute of Geological & Nuclear Sciences Ltd, Lower Hutt, New Zealand.
Stewart, M.K., 2012, A 40-year record of carbon-14 and tritium in the Christchurch groundwater system, New Zealand: Dating of young samples with carbon-14: Journal of Hydrology, v. 430-431, p. 50–68, doi: 10.1016/j.jhydrol.2012.01.046.
Taylor, C.B., Wilson, D.D., Brown, L.J., Stewart, M.K., Burden, R.J., and Brailsford, G.W., 1989, Sources and Flow of North Canterbury Plains Groundwater, New Zealand: Journal of Hydrology, v. 106, no. 3-4, p. 311–340, doi: 10.1016/0022-1694(89)90078-4.
Tenthorey, E., and Fitz Gerald, J.D., 2006, Feedbacks between deformation, hydrothermal reaction and permeability evolution in the crust: Experimental insights: Earth and Planetary Science Letters, v. 247, no. 1-2, p. 117–129, doi: 10.1016/j.epsl.2006.05.005.
Thain, I., Reyes, A.G., and Hunt, T., 2006, A practical guide to exploiting low temperature geothermal resources:.
Timm, C., Hoernle, K., van den Bogaard, P., Bindeman, I., and Weaver, S., 2009, Geochemical evolution of intraplate volcanism at Banks Peninsula, New Zealand: Interaction between asthenospheric and lithospheric melts: Journal of Petrology, v. 50, no. 6, p. 989–1023, doi: 10.1093/petrology/egp029.
Timm, C., Hoernle, K., Werner, R., Hauff, F., Van den Bogaard, P., White, J., Mortimer, N., and Garbe-Schönberg, D., 2010, Temporal and geochemical evolution of the Cenozoic intraplate volcanism of Zealandia: Earth-Science Reviews, v. 98, no. 1-2, p. 38–64, doi: 10.1016/j.earscirev.2009.10.002.
Tonkin & Taylor Report 52010.040, 2011,.
USGS, 2012, Alkalinity Calculator:.
USGS, 2013, Methods for Alkalinity Calculations:.
Wannamaker, P.E., 2002, Fluid generation and pathways beneath an active compressional orogen, the New Zealand Southern Alps, inferred from magnetotelluric data: Journal of Geophysical Research, v. 107, no. B6, p. 1–21, doi: 10.1029/2001JB000186.

9 APPENDIX

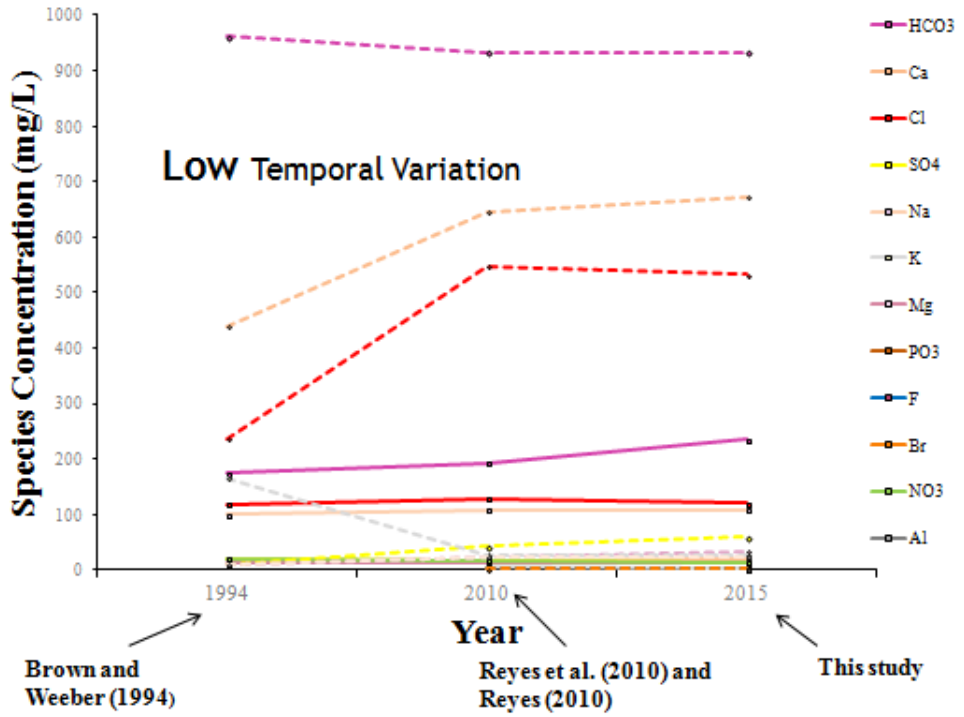

Appendix 8: Temporal variation of Banks Peninsula warm springs. Results compare samples from Motukarara (solid lines) and Rapaki Bay (dashed lines). data gathered from this study, Brown and Weeber (1994), Reyes (2010), and Reyes et al. (2010).

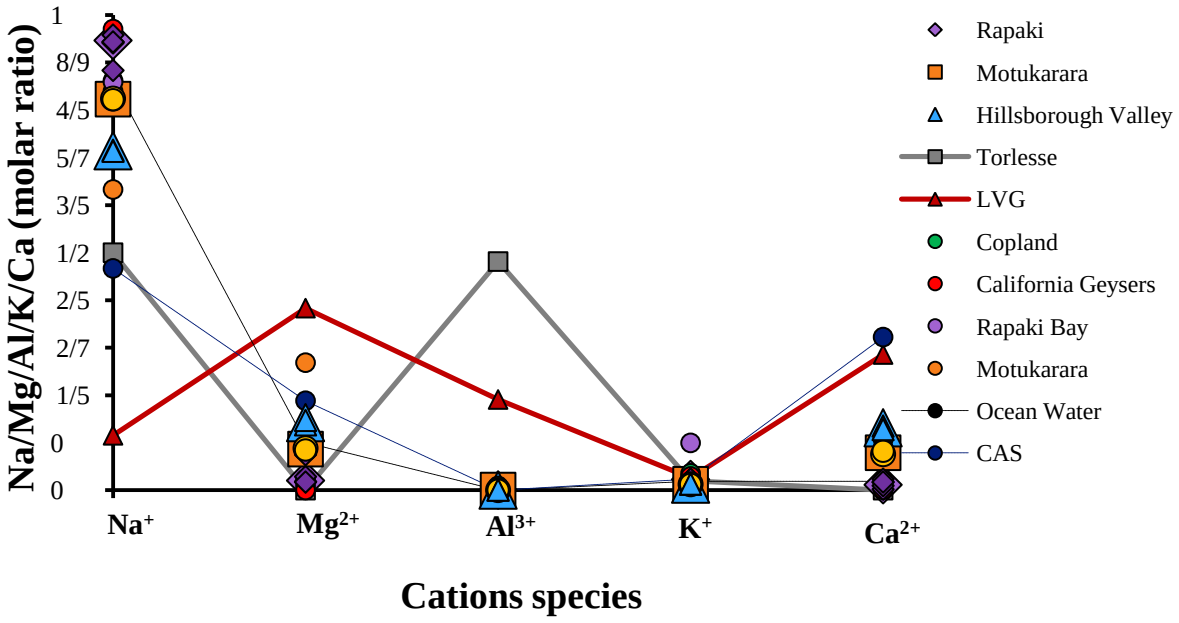

Appendix 9: Comparison of Banks Peninsula warm spring water against rock type, comparable sources, and influential waters. Banks Peninsula waters exhibit greater similarities to the torlesse than Lyttelton Volcanic Group (LVG). Molar ratios of the major cation species reveal similar trends to other metamorphic hydrothermal meteoric origin waters. Additional data from Donnelly-Nolan et al. (1993), Brown and Weeber (1994), Bierlein and Craw (2009), Timm et al. (2009), Reyes et al. (2010), and Cox et al. (2015).

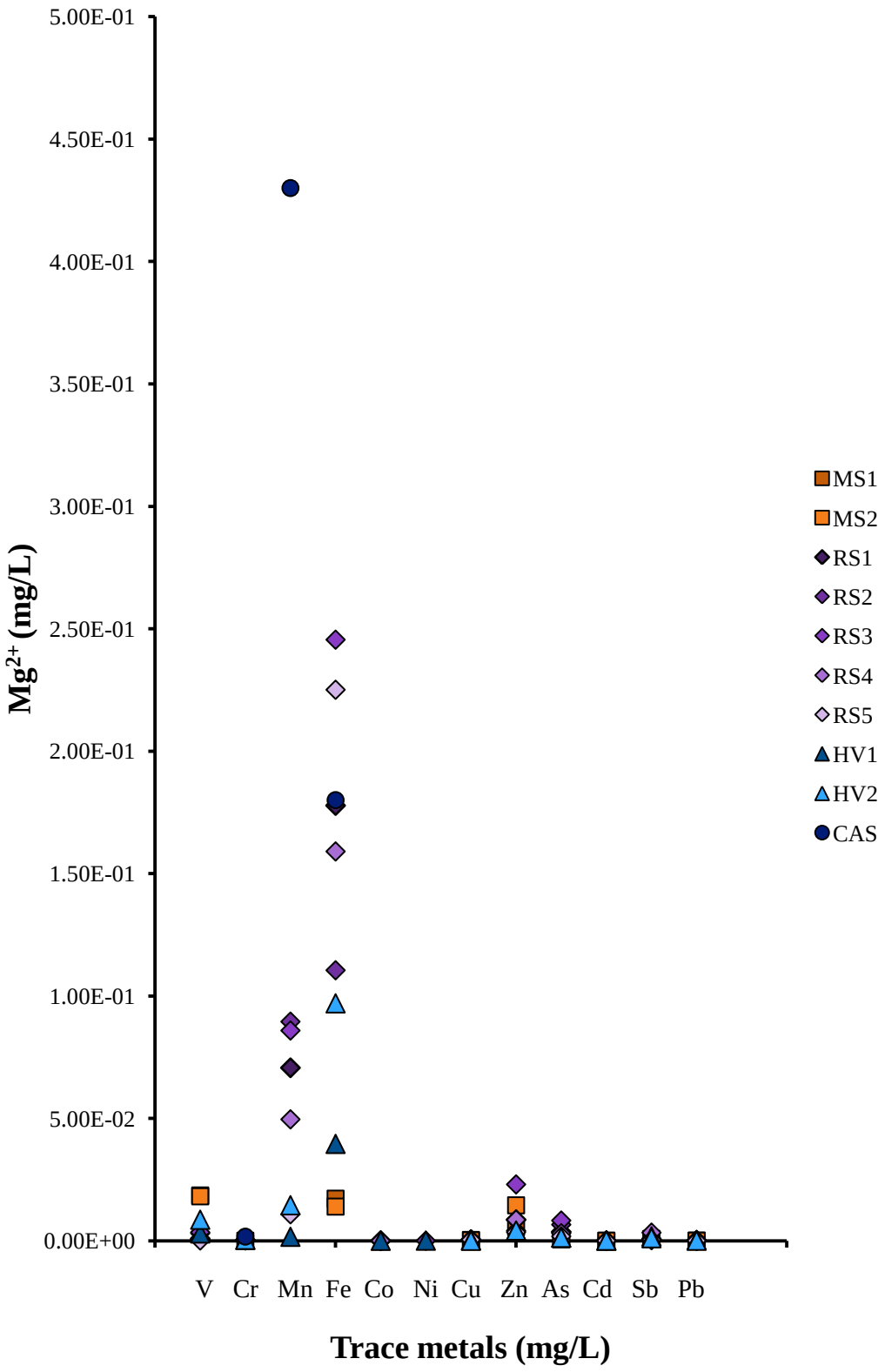

Appendix 10: Trace metal analysis of Banks Peninsula warm springs compared to the Canterbury Aquifer System (CAS) (Hayward, 2002). The warm springs do not exhibit any trends relative to the CAS.

Appendix 11: CRDS soil-gas flux data

	CRDS					
Sample	CO2 Method	Flux	$\delta^{13}C$	CH4 Method	Flux	$\delta^{13}C$
1	LR	1.760 ± 0.023	-18.441			
2	LR	11.363 ± 0.047	-14.544	HMR	0.409 ± 0.007	-56.288
3	LR	2.639 ± 0.030	-17.637			
4	HMR	5.384 ± 0.066	-16.448	LR	0.111 ± 0.0004	-54.196
5	LR	2.200 ± 0.025	-30.514			
6	LR	2.197 ± 0.015	-15.005			
7	HMR	39.694 ± 1.588	-14.655	HMR	32.894 ± 2.667	-59.965
8	HMR	3.210 ± 0.113	-13.568			
9	HMR	1.265 ± 0.050	-17.633			
10	LR	0.965 ± 0.034	-20.919			
11	LR	1.283 ± 0.012	-19.667			
12	LR	20 ± 0.049	-20.672			
13	HMR	12 ± 0.051	-25.181			
14	HMR	20 ± 0.067	-20.285	HMR	1 ± 0.0006	-64.701
15	HMR	25 ± 0.066	-32.016	HMR	1 ± 0.0007	-63.192
16	HMR	25 ± 0.052	-23.842	HMR	0.133 ± 0.0003	-58.665
17	HMR	13.3 ± 0.019	-22.177			
18	HMR	1.7143 ± 0.011	-18.610			
19	LR	0.1333 ± 0.013	-7.162			
20	HMR	0.7143 ± 0.009	-19.937			
21	LR	0.1714 ± 0.014	-19.486			
22	HMR	0.4 ± 0.003	-18.521			
23	LR	0.1667 ± 0.008	-20.070			
24	HMR	0.1333 ± 0.010	-26.685			
25	HMR	2 ± 0.026	-18.138	HMR	3.5 ± 0.004	-59.669
26	LR	1.2 ± 0.049	-24.737			
27	HMR	0.1 ± 0.009	-18.370			
28	LR	0.08 ±0.005	-19.791			

Appendix 12: IRGA soil-gas flux data

	IRGA					
Sample	CO2 Method	Flux	$\delta^{13}C$	CH4 Method	Flux	$\delta^{13}C$
1	LR	1.426 ± 0.023	-18.441			
2	HMR	12.133 ± 0.125	-14.544			
3	LR	2.506 ± 0.014	-17.637			
4	HMR	4.943 ± 0.077	-16.448			
5	HMR	2.353 ± 0.057	-30.514			
6	LR	2.045 ± 0.017	-15.005			
7	HMR	31.241 ± 1.395	-14.655	HMR	31.027 ± 1.503	-59.965
8						
9	HMR	0.917 ± 0.052	-17.633			
10	LR	0.976 ± 0.017	-20.919			
11	LR	1.255 ± 0.013	-19.667			

Appendix 13: Council signposts at Rapaki Bay; a potential contaminant source for rain sample RBR